SLAC–PUB–7634
UPR–788–T

Bounds on Supersymmetry from Electroweak Precision Analysis

Jens Erler*
Department of Physics and Astronomy
University of Pennsylvania
Philadelphia, PA 19104

Damien M. Pierce†
Stanford Linear Accelerator Center
Stanford University
Stanford, CA 94309

Abstract

The Standard Model global fit to precision data is excellent. The Minimal Supersymmetric Standard Model can also fit the data well, though not as well as the Standard Model. At best, supersymmetric contributions either decouple or only slightly decrease the total χ^2, at the expense of decreasing the number of degrees of freedom. In general, regions of parameter space with large supersymmetric corrections from light superpartners are associated with poor fits to the data. We contrast results of a simple (oblique) approximation with full one-loop results, and show that for the most important observables the non-oblique corrections can be larger than the oblique corrections, and must be taken into account. We elucidate the regions of parameter space in both gravity- and gauge-mediated models which are excluded. Significant regions of parameter space are excluded, especially with positive supersymmetric mass parameter μ. We give a complete listing of the bounds on all the superpartner and Higgs boson masses. For either sign of μ, and for all supersymmetric models considered, we set a lower limit on the mass of the lightest CP–even Higgs scalar, $m_h \geq 78$ GeV. Also, the first and second generation squark masses are constrained to be above 280 (325) GeV in the supergravity (gauge-mediated) model.

*e-mail: erler@langacker.hep.upenn.edu
†e-mail: pierce@slac.stanford.edu

1 Introduction

For more than a decade, ideas involving supersymmetry (SUSY) have been among the most popular extensions of the Standard Model (SM), having the greatest potential to solve its shortcomings such as the gauge hierarchy problem and the lack of a quantized version of gravity. Indeed, all superstring theories necessarily contain quantum gravity and supersymmetry. Moreover, very recently, using arguments based on various dualities and supersymmetry, all superstring theories as well as 11 dimensional supergravity seem to be connected nonperturbatively [1], suggesting a unified theory in which supersymmetry is one of the indispensable key elements. The idea of supersymmetric unification is further supported by the observation of gauge coupling unification [2] two orders of magnitude below the reduced Planck scale, $M_P/\sqrt{8\pi} \sim 2 \times 10^{18}$ GeV, the natural supergravity scale.

Taken together this implies a strong motivation to investigate the phenomenological consequences of low energy supersymmetry. In this paper we present a systematic study of precision observables in the minimal supersymmetric standard model (MSSM) in an attempt to find favorable and/or excluded regions in SUSY parameter space. We do this in two scenarios for how supersymmetry breaking is conveyed to the observable sector.

In the "minimal supergravity" model [3] supersymmetry breaking is transmitted from a hidden sector to the observable sector via gravitational interactions. Supersymmetry is spontaneously broken in the hidden sector at a scale Λ [4]. In popular models which invoke gaugino condensation [5], $\Lambda \sim (M_P^2 M_{SUSY}/8\pi)^{1/3} \sim 10^{13}$ GeV. Since gravity is flavor blind, it is assumed that the explicit soft breaking terms in the observable sector are universal at the supergravity scale.

In simple models of gauge mediation [6] there is a supersymmetry breaking sector which gives rise to both an F-term, F_X, and a vacuum expectation value, X, of a standard model singlet field. This field is coupled to the vector-like "messenger fields", M, through a superpotential interaction of the form $\lambda X M \overline{M}$. The generated soft mass term for a given superpartner is proportional to $\Lambda \equiv F_X/X \sim 4\pi M_Z/\alpha \sim 10^5$ GeV, and grows with the square of its gauge couplings. Therefore sleptons are much lighter than squarks and the gluino is heavier than charginos and neutralinos.

In both cases the generated soft terms are sufficiently flavor universal that all flavor changing neutral current (FCNC) effects are adequately suppressed. However, in the minimal supergravity model it must be implicitly assumed that universality is not spoiled by the Kähler potential.

Recently, a number of articles [7] examined whether supersymmetry has the potential to describe the data better than the SM. The conclusions in the affirmative were mainly driven by R_b (see section 2), which at times was more than 3σ higher than SM expectations. Loops involving light charginos and top squarks could account for a large part of the discrepancy for low $\tan\beta$, provided the effect was not canceled by charged-Higgs loops. For large $\tan\beta$, large shifts could be obtained from loops containing bottom quarks and light neutral Higgs bosons, and to a lesser extent from neutralino/bottom-squark loops. However, more recent analyses find the measured value of R_b closer to the SM prediction (the discrepancy is 1.3σ), and at the same time direct limits on superpartner masses have increased. Now, even if one is able to find a region of parameter space where the R_b discrepancy is alleviated, the decrease in the overall χ^2 is not significant. Also, in those regions of parameter space one typically finds that the discrepancy in $A^{FB}(b)$ is made worse. In the specific high-scale models of supersymmetry breaking we consider in this paper, the largest possible shift in R_b is less than 1σ. It follows that R_b now plays a much smaller role, and supersymmetric models can no longer yield significantly smaller values of χ^2 than the SM.

Therefore, in this work we take a different point of view[1] and focus on elucidating the excluded regions of supersymmetry parameter space. We present a complete one-loop analysis of supersymmetry, combined with a state of the art SM calculation. Input data are as of August 1997.

In Section 2 we give a short overview of the inputs and observables we use. For reference we perform a global fit to the SM, and comment on some of the deviating observables. Section 3 describes the parameter spaces of the supersymmetric models in more detail, and reviews recent direct limits on superpartner masses. We compare the oblique approximation [12] with the full calculation in some detail. We present our results in Section 4 and our conclusions in Section 5.

2 Overview

Within the SM we perform a global fit to a total of 31 observables listed below. We include full one-loop radiative corrections [13]; full QCD corrections up to $\mathcal{O}(\alpha_s^3)$; higher order QCD corrections when enhanced by beta function effects; mixed electroweak/QCD corrections of $\mathcal{O}(\alpha\alpha_s)$ with the exception of non-leading special vertex corrections to $Z \to b\bar{b}$ decays[2]; and $\mathcal{O}(\alpha^2)$ corrections when enhanced, e.g. by large top mass effects or large logarithms.

The Fermi constant, G_μ, and the fine structure constant, α, are taken as fixed inputs. The five fit parameters are the strong coupling constant, α_s; the contribution of the five light quarks to the photon vacuum polarization function, $\Delta\alpha_{\rm had}^{(5)}$; and the masses of the Z-boson, M_Z, the Higgs scalar, M_H, and the top quark, m_t. Alternatively, one may fix M_Z as well, since its relative error is now comparable to that of G_μ. We have chosen to leave it free, because the Z-mass measurement is correlated with other observables. In practice, the difference between the two treatments is numerically insignificant. We have organized the measurements into seven groups:

- **9 lineshape observables**

  The mutually correlated LEP observables [16] are determined from a common fit to the Z lineshape and the leptonic forward-backward asymmetries. They include the Z-boson pole mass M_Z, the total Z-width Γ_Z, the hadronic peak cross section,

  $$\sigma^0_{\rm had} = \frac{12\pi}{M_Z^2}\frac{\Gamma_{ee}\Gamma_{\rm had}}{\Gamma_Z^2} ,$$

  and, for each lepton flavor, $\ell = e,\ \mu,\ \tau$, the ratios $R_\ell = \Gamma_{\rm had}/\Gamma_{\ell\ell}$, and the pole asymme-

[1] First results of this kind of analysis were presented in Ref. [8].

[2] These have been calculated very recently and shown to be quite small compared to the analogous corrections to the lighter quark vertices [15].

tries, $A^{FB}(\ell)$. Γ_x denotes the partial Z width into x. Defining

$$A_f = \frac{1 - 4Q_f \sin^2\theta^f_{\rm eff}}{1 - 4Q_f \sin^2\theta^f_{\rm eff} + 8Q_f^2 \sin^4\theta^f_{\rm eff}} \ ,$$

where $\sin^2\theta^f_{\rm eff}$ is the effective weak mixing angle for fermion f at the Z scale, we have

$$A^{FB}(f) = \frac{3}{4} A_e A_f \ .$$

- **3 further LEP asymmetries**

  These are the τ polarization, $\mathcal{P}(\tau) = A_\tau$, its forward-backward asymmetry, $\mathcal{P}^{FB}(\tau) = A_e$, and the hadronic charge asymmetry, $\langle Q^{FB}\rangle$, which is quoted as a measurement of $\sin^2\theta^e_{\rm eff}$ [16].

- **6 heavy flavor observables**

  The mutually correlated heavy flavor observables from LEP and SLC [16] are the ratios $R_q = \Gamma_{q\bar q}/\Gamma_{\rm had}$; the forward-backward pole asymmetries, $A^{FB}(q)$ (LEP); and the combined left-right forward-backward asymmetries, $A^{FB}_{LR}(q) = A_q$ (SLC), each for $q = b, c$.

- **3 further SLD asymmetries**

  These are the very precise measurement of the left-right asymmetry for hadronic final states [17], $A_{LR}(\text{had}) = A_e$; the analogous $A_{LR}(\mu,\tau) = A_e$, which is obtained from a common fit including polarized Bhabha scattering [18]; the left-right forward-backward asymmetries [18], $A^{FB}_{LR}(\ell) = A_\ell$ for $\ell = \mu$ or τ; and the hadronic charge flow asymmetry [19], $A_Q = A_e$, which is basically the ratio of weighted forward-backward and left-right forward-backward asymmetries[3]. We combine the 3 values of A_e from SLD into one number,

  $$A_e = 0.1548 \pm 0.0033 \ .$$

- **2 pole masses**

  We combine the W-mass measurements from CDF [20], DØ [21] and UA2 [22], $M_W(p\bar p) = 80.409 \pm 0.090$ GeV, with the one from LEP 2 [16], $M_W(\text{LEP}) = 80.481 \pm 0.140$ GeV, obtaining

  $$M_W(\text{world}) = 80.430 \pm 0.076 \text{ GeV}.$$

  Combining the results of all top decay channels at CDF [23] and DØ [24], we find

  $$m_t = 175 \pm 5 \text{ GeV}.$$

  We fix the scale invariant $\overline{\rm MS}$ masses for the heavy quarks, $\overline{m}_b(\overline{m}_b) = 4.33$ GeV and $\overline{m}_c(\overline{m}_c) = 1.30$ GeV.

[3]Since $A_{LR}(\text{had})$ is proportional to the electron beam polarization, $\mathcal{P}_e$, while A_Q is inversely proportional, the geometric mean of the two determinations yields A_e independently of $\mathcal{P}_e$. The result [19] is $A_e = 0.1574 \pm 0.0208$, or equivalently, $\sin^2\theta^e_{\rm eff} = 0.2302 \pm 0.0027$.

- **6 low energy observables**

  The weak charge from atomic parity violation (APV) in Tl has been measured by groups in Oxford [25] and Seattle [26], $Q_W(^{205}\mathrm{Tl}) = -114.77 \pm 1.23 \pm 3.44$, and in Cs by the Boulder group [27], $Q_W(^{133}\mathrm{Cs}) = -72.11 \pm 0.27 \pm 0.89$, where the first errors are experimental and the second theoretical. The recent result of the deep inelastic scattering (DIS) experiment of CCFR [28] is combined with the measurements of CDHS [29] and CHARM [30], yielding $\kappa = 0.5805 \pm 0.0039$, where κ is a linear combination of effective 4-Fermi operator coefficients. Similarly, $\nu_\mu e$ scattering experiments, dominated by the recent CHARM II results [31], yield determinations of leptonic 4-Fermi operator coefficients, $g_V^{\nu e} = -0.041 \pm 0.015$ and $g_A^{\nu e} = -0.507 \pm 0.014$. The CLEO measurement of $B \to X_s\gamma$ [33] yields the 90% confidence interval,

  $$1 \times 10^{-4} < B(B \to X_s\gamma) < 4.2 \times 10^{-4}.$$

  When a variable is defined in a finite interval (here between 0 and 1), and a boundary of the interval is within a few standard deviations from the central value, a variable transformation should be performed such that the new variable is defined on the whole real axis. Arguments analogous to the ones supporting a flat prior distribution in $\log M_H$ rather than in M_H (see next section) lead to the logistic transformation[4], $\mathrm{lg}(x) = \ln(x/(1-x))$ [34]. This results in a more Gaussian shaped distribution, and in our case, in a more (less) conservative assessment of the upper (lower) error bar. The $b \to s\gamma$ amplitude can receive very large contributions from the leading-order supersymmetric loops, and the next-to-leading order corrections (which have not been calculated) could be important. The uncertainty in the large and positive MSSM contributions is taken into account by the more conservative treatment of the upper error bar. Additionally, because of these uncertainties, we have chosen the more conservative of the two error estimates in Ref. [33], which is obtained by adding the statistical and systematic errors linearly. Compared to this experimental error, the theoretical error due to QCD uncertainties in the SM prediction [65, 35] can be neglected.

- **2 gauge couplings**

  We use the constraint $\Delta\alpha_{\mathrm{had}}^{(5)} = 0.02817 \pm 0.00062$ [36]. We also include the external constraint $\alpha_s = 0.118 \pm 0.003$, which we obtained by combining non-Z lineshape determinations of α_s [37]. In this case we have doubled all theoretical errors to account for ignored correlations, and because these are by far the most difficult to estimate and very non-Gaussian in nature.

The best fit values of the SM input parameters are shown in Table 1. The χ^2/d.o.f. of the fit is 26.6/26, corresponding to an almost perfect fit with a goodness (probability of larger χ^2) of 43%. Our results differ from the ones quoted by the LEP Electroweak Working Group [16]. The differences can be traced to a different treatment of radiative corrections and to a slightly different and more recent data set. Most importantly, inclusion of $\mathcal{O}(\alpha^2 m_t^2)$ corrections [38] shift the extracted M_H by -17 GeV, and $\mathcal{O}(\alpha\alpha_s)$ vertex corrections [15, 39] increase the

[4] Equivalently, one may continue to use the old variable and include a nontrivial weight factor (the Jacobian) $1/[x(1-x)]$.

m_t	172 ± 5 GeV
M_H	66^{+74}_{-38} GeV
M_Z	91.1867 ± 0.0020 GeV
$\alpha_s(M_Z)$	0.1195 ± 0.0022
$\Delta\alpha^{(5)}_{\rm had}$	0.02817 ± 0.00064

Table 1: Results for the SM fit parameters.

extracted α_s by 0.001. Taking these and other smaller differences, which are well understood, into account, the agreement with the results of the LEPEWWG is excellent[5]. Our results are in close correspondence with the very recent update of the Particle Data Group [13]; one major difference is the external α_s constraint. Also, here M_H is allowed as a free parameter, in which case the SM best fit value of M_H is below the lower limit from direct searches. In the MSSM the bound is relaxed to $m_h \gtrsim 60$ GeV [40], consistent with the central value in Table 1.

We list the measured values of all the observables in Table 2, together with their global best fit values. The pull, defined as the difference between the measurement and the fit result divided by the experimental error, is also shown. The agreement is excellent. The two largest discrepancies are only at the 2σ level.

Based on all data from 1992–1996, the left-right asymmetry, $A_{LR}(\text{had}) = 0.1550 \pm 0.0034$, is now closer to the Standard Model expectation of 0.147 ± 0.002 than previously [17]. However, because of the smaller error, A_{LR} is still significantly above the Standard Model prediction. There is also an experimental difference of $\sim 1.9\sigma$ between the SLD value of A_ℓ (SLD) $= 0.1547 \pm 0.0032$ from all A_{LR} and $A^{FB}_{LR}(\ell)$ data on one hand, and the LEP value A_ℓ (LEP) $= 0.1461 \pm 0.0033$ obtained from $A^{FB}(\ell)$, $A_e(\mathcal{P}_\tau)$, and $A_\tau(\mathcal{P}_\tau)$ on the other hand, in both cases assuming lepton-family universality.

Relaxing universality, one can extract the various A_f in a model independent way. First, we combine A_e from $A^{FB}(e)$ and $\mathcal{P}^{FB}(\tau)$ with the value from the SLC to obtain $A_e = 0.1518 \pm 0.0029$. This value for A_e can now be used to extract the other A_f from forward-backward asymmetries. Looking at Table 2 one sees that all 3 observables which are sensitive to the τ-vertex, namely $A^{FB}(\tau)$, $\mathcal{P}(\tau)$, and $A^{FB}_{LR}(\tau)$, deviate by 1σ or more. However, when combined, one finds $A_\tau = 0.1448 \pm 0.0059$, in excellent agreement with the SM value of 0.147 ± 0.002. At present, it seems more likely that we are facing an experimental discrepancy. Using $A^{FB}(f)$ from LEP and $A^{FB}_{LR}(f)$ from the SLC for $f = \mu$, b, and c, we find that A_μ and A_c are consistent with each other and the SM. On the other hand, while the A_b determinations are also consistent with each other, their combined value, $A_b = 0.872 \pm 0.024$, deviates 2.6σ from the SM value of 0.935. A similar analysis assuming lepton universality yields [16] $A_b = 0.877 \pm 0.023$ which is 2.5σ low. One can also obtain $A_e = 0.148 \pm 0.002$ from a global fit excluding the quark sector[6], and derive $A_b = 0.888 \pm 0.022$, still a 2.1σ deviation. We can therefore conclude that the data show an anomaly in A_b, independently of exactly how it is extracted. However, this deviation of about 6% cannot be due to supersymmetric loops since a 30% correction to $\hat\kappa_b$ (defined by $\sin^2\theta^b_{\rm eff} = \hat\kappa_b \sin^2\hat\theta_{\overline{\rm MS}}$) would be necessary to account for the central value of

[5]See also 'note added' at the end.

[6]Here we have fixed $M_H = M_Z$ because otherwise the Higgs mass is driven to very low (excluded) values.

A_b. Only a new contribution at tree level which does not contradict R_b (including the off-peak R_b measurements by DELPHI [41]), can conceivably account for such a low A_b [42]. In particular, a τ-sneutrino with mass close to M_Z and R-parity violating couplings is a natural candidate [43]. Of course, supersymmetry can also affect $A^{FB}(b)$ through the weak mixing angle in the A_e factor. Such a correction can not, however, help to resolve the LEP/SLC A_ℓ discrepancy.

This discussion and the remarks about R_b in the introduction show that we cannot expect that the inclusion of supersymmetric loops will significantly improve the goodness of the fit to electroweak data. On the contrary, there are regions in parameter space where the fit is quite poor, and those regions must be ruled out. Here we do not test the supersymmetry hypothesis. Rather, the primary goal of our analysis must be to identify the excluded regions of supersymmetry parameter space.

3 Supersymmetry

In gravity-mediated models supersymmetry is broken in a hidden sector and the breaking is communicated to the observable sector through supergravity effects. This transmission is suppressed by inverse powers of the Planck mass. The assumption of a flat Kähler metric for the fields in the observable sector (an assumption which can be called into question) yields a universal scalar mass, M_0, a universal gaugino mass, $M_{1/2}$, and a universal trilinear scalar coupling, A_0, at the Planck scale [44]. In the minimal supergravity model we impose this universality at the scale where the (U(1) and SU(2)) gauge couplings unify, $M_{\rm GUT} \sim 2 \times 10^{16}$ GeV. The running of the soft parameters from M_P to $M_{\rm GUT}$ should in general be taken into account [45], but it is model dependent, so it is ignored in the minimal supergravity model.

From the inputs M_Z, G_μ, α, $\Delta\alpha^{(5)}_{\rm had}$, and α_s, and the fermion masses m_t, m_b, and m_τ, we determine the full one-loop values of the gauge and Yukawa couplings at the Z-scale. We then solve the set of coupled two-loop renormalization group equations (RGE's) for the couplings and soft parameters by iteration. This set of differential equations has two-sided boundary conditions: the hard parameters (gauge and Yukawa couplings) are fixed at the Z-scale and the soft parameters are fixed at the unification scale. In each iteration we impose electroweak symmetry breaking at the squark scale. This occurs naturally, as the large top-quark Yukawa coupling drives the Higgs mass-squared $m^2_{H_2}$ negative. The electroweak symmetry breaking conditions allow us to solve for the Higgsino mass-squared, μ^2, and the CP–odd Higgs boson mass-squared, m^2_A. These are determined as functions of $\tan\beta$, the ratio of vacuum expectation values, to full one-loop order [10]. To summarize, the minimal supergravity model parameter space is specified by

$$M_0,\ M_{1/2},\ A_0,\ \tan\beta,\ \text{and}\ \mathrm{sgn}(\mu)\ . \tag{1}$$

Just as in minimal supergravity, simple models of gauge-mediated supersymmetry breaking also introduce a hidden sector in which supersymmetry is dynamically broken, so that for one (or more) hidden sector fields X, $F_X \neq 0$. Here, however, the messenger fields which couple to X are assumed to be charged under the SM gauge group. As a result, supersymmetry breaking is transmitted through messenger loop effects, and observable fields receive soft masses roughly proportional to the square of their gauge couplings. It follows that scalars with identical quantum numbers are mass degenerate, and FCNC effects are sufficiently suppressed as long as the messenger scale $M = \lambda X \lesssim 10^{15}$ GeV [46]. The key parameter here is $\Lambda = F_X/X$, as this parameter sets the scale of the entire superpartner spectrum. The messenger scale M determines the amount of RGE evolution, and therefore enters only logarithmically. As before, radiative electroweak symmetry breaking occurs rather generically over the parameter space. It is generally difficult to arrange for the right magnitude of μ and the soft supersymmetry breaking parameter B, but solutions to this problem exist [47]. We assume that the mechanism which is responsible for generating B and μ does not at the same time give extra contributions to the soft Higgs, squark and slepton masses. The superpartner spectrum depends on the representation(s) of the messenger sector. We consider the cases where the messenger sector is comprised of a $\mathbf{5} + \overline{\mathbf{5}}$ pair of fields, or a $\mathbf{10} + \overline{\mathbf{10}}$ pair[7]. For the purpose of our analysis a $\mathbf{10} + \overline{\mathbf{10}}$ messenger sector is equivalent to a model with three $\mathbf{5} + \overline{\mathbf{5}}$ pairs. In the minimal gauge-mediated model the supersymmetry parameter space includes

$$M,\ \Lambda,\ \tan\beta,\ \text{and}\ \mathrm{sgn}(\mu), \tag{2}$$

with $\Lambda < M$ to ensure the absence of gauge symmetry breaking in the messenger sector. The A-terms are generated at a higher order in perturbation theory, and are expected to be $\mathcal{O}(\alpha/\pi)$ relative to the gaugino masses. Hence, we set $A = 0$ at the messenger scale. This results in relatively small squark mixing.

In either supersymmetry model, we proceed by randomly picking a point in its parameter space, Eq. (1) or Eq. (2). For an initial set of values for the *standard parameters*, M_Z, m_t, α_s and $\Delta\alpha^{(5)}_{\rm had}$, we then solve the model, i.e. we self-consistently evaluate the soft parameters at the weak scale, and compute the physical superpartner and Higgs-boson masses, couplings and mixings[8]. This enables us to compute the full supersymmetric one-loop corrections [10, 48, 49] to each observable[9], and to perform a χ^2 minimization with respect to the standard parameters. We iterate the solution of the supersymmetric model for the best fit values of the standard parameters until this process has converged. On the last iteration we require that the full one-loop electroweak symmetry breaking conditions are satisfied, and impose that the Yukawa couplings remain perturbative ($\lambda^2/4\pi < 1$) up to $M_{\rm GUT}$.

Finally, we apply the direct lower limits on superpartner and Higgs boson masses. Searches at LEP constrain the mass of the CP–odd Higgs boson, A, to be larger than 62.5 GeV, and that of the lightest CP–even Higgs scalar, h, to be heavier than 62.5 GeV for small m_A, or 70.7 GeV for large m_A [50]. There are mass limits from LEP 2 on charginos ($m_{\tilde\chi^+} > 91$ GeV) [51], selectrons ($m_{\tilde e} > 76$ GeV), smuons ($m_{\tilde\mu} > 59$ GeV), staus ($m_{\tilde\tau} > 53$ GeV) [52], and stops ($m_{\tilde t} > 65$ GeV) [53] provided these superpartners are not nearly degenerate with the lightest neutralino, $\tilde\chi^0_1$. The chargino limit is slightly degraded if the electron sneutrino is light. The top squark limit is for the case when it decouples from the Z, and increases to 72 GeV for no left-right mixing. For a relatively light $\tilde\chi^0_1$, DØ excludes top squarks up to 95 GeV [54]. In the gauge-mediated models the next-to-lightest supersymmetric particle (NLSP) can be a slepton. We assume in these models that the NLSP decays outside the detector, in which case

[7] The messenger fields are assumed to come in complete $SU(5)$ representations to preserve the successful gauge coupling unification. An actual $SU(5)$ symmetry, however, is not assumed.

[8] We compute the light Higgs mass in a full one-loop (diagrammatic) calculation [10].

[9] For the low-energy observables from atomic parity violation, deep inelastic scattering, and neutrino scattering, we work in the oblique approximation. For these observables the non-oblique supersymmetric corrections are expected to be negligible relative to the experimental errors.

the search limits for stable charged particles apply, which are $m_{\tilde{\ell}} > 67$ (69) GeV for right-handed (left-handed) sleptons [55]. The for us relevant CDF searches [56] suggest for first and second generation squarks, $m_{\tilde{q}} > 210$ GeV, and for gluinos, $m_{\tilde{g}} > 173$, but these limits do not apply uniformly over parameter space. Therefore we impose relaxed limits of 200 and 160 GeV, respectively. However, it turns out that in the models we consider the direct limits on squark and gluino masses are for the most part irrelevant. Once the other mass limits are taken into account, the smallest possible squark (gluino) masses vary from 210 (230) to 370 (330) GeV, depending on the model.

At each point in our scan over parameter space we apply the constraints from electroweak symmetry breaking, Yukawa perturbativity, and the direct searches. If any of these checks fail, the point is disregarded. We refer to a point in the supersymmetry parameter space which passes these tests as a *quaint point*. The set of points which pass comprise the *quaint parameter space*.

We now discuss the interpretation of the resulting χ^2 value for a given quaint point. It is important to notice that the overall χ^2 value is relevant only for hypothesis testing. As noted before, this is not our goal. We derive our confidence that the study of low-energy supersymmetry is worthwhile from other (more indirect) arguments. Rather, we will address the question of preferred or disfavored quaint regions. Before we continue to defend our procedure, we would like to compare our situation with the SM Higgs mass.

In standard analyses, the quoted limits on M_H are independent of the χ^2 value of the SM best fit. A standard (Bayesian) procedure is to determine the *posterior probability distribution function* (posterior p.d.f.) as the product of the *prior p.d.f.* (prior) and the likelihood function (here $\sim \exp(-\chi^2/2)$). The choice of a prior is always made, but is oftentimes obscured. In the case of M_H, a *non-informative* prior is desired, or perhaps an informative prior which accounts for the direct lower limit, and is non-informative otherwise. The choice of a suitable prior is not unique[10]. A non-informative prior is by no means necessarily flat (constant); in general a flat prior ceases to be constant after a variable transformation introduces a non-trivial Jacobian. Clearly, such a variable transformation cannot change the results of a statistical analysis unless the Jacobian is dropped. In the case of M_H, one often chooses a prior which is flat in $\log M_H$. There are various ways to justify this choice [34]. One rationale is that a flat distribution is most natural for a variable defined over the real numbers. This is the case for $\log M_H$ but not M_H^2. Another complication arises since flat priors in both $\log M_H$ and M_H^2 are improper, i.e. their integrals are divergent and cannot be normalized. This is not necessarily problematic as long as the likelihood function is sufficiently convergent so that the posterior p.d.f. is normalizable. For M_H this is the case, due to the non-decoupling property of the SM Higgs boson corrections.

In the case of supersymmetry, however, the posterior p.d.f. remains improper, because superpartners and the heavy Higgs doublet decouple, and the likelihood function is asymptotically finite. To cope with this problem one might

- cut superparticle masses or soft parameters off somewhere in the TeV region, arguing that higher scales are unnatural and incompatible with the primary motivations for low-energy supersymmetry such as the hierarchy problem. In other words one would

[10] The sensitivity of the posterior p.d.f. to the (non-informative) prior diminishes rapidly with the inclusion of more data.

introduce an informative prior. However, conclusions would directly depend on the precise choice of the cut-off scale, i.e. the prior;

- choose a more sophisticated informative prior which utilizes fine-tuning criteria in order to produce a proper posterior p.d.f. While aesthetically appealing in particular from a Bayesian viewpoint[57], the implementation would be rather involved and computationally expensive. Also the establishment of an appropriate fine-tuning criteria is not unique [58];

- exclude all quaint points which have a $\Delta\chi^2 = \chi^2 - \chi^2_{\rm min} > 3.84$, where $\chi^2_{\rm min}$ is the minimum value of χ^2 in the supersymmetry model under consideration. In a univariate Gaussian situation this procedure corresponds to the 95% CL. It lacks the conceptual rigor of Bayesian statistics, but has the advantage of being independent of the specification of prior information. We will use this criterion in our analysis.

Before showing the results of the full one-loop analysis, we discuss the results obtained in the oblique approximation. For some observables the dominant supersymmetric corrections are of oblique type, i.e. they arise from vector-boson self-energy diagrams and can be described by the S, T and U parameters[11] [12],

$$\begin{aligned}
S &= \left[\cos^2\theta_W\,(F_{ZZ} - F_{\gamma\gamma}) - \frac{\cos\theta_W}{\sin\theta_W}\cos 2\theta_W F_{\gamma Z}\right] \times \frac{4\sin^2\theta_W}{\alpha}\,, \\
T &= \left[\frac{\Pi_{WW}(0)}{M_W^2} - \frac{\Pi_{ZZ}(0)}{M_Z^2} - 2\frac{\sin\theta_W}{\cos\theta_W}\frac{\Pi_{\gamma Z}(0)}{M_Z^2}\right] \times \frac{1}{\alpha}\,, \\
U &= \left[F_{WW} - \cos^2\theta_W F_{ZZ} - \sin^2\theta_W F_{\gamma\gamma} - \sin 2\theta_W F_{\gamma Z}\right] \times \frac{4\sin^2\theta_W}{\alpha}
\end{aligned}$$

where $F_{ij} = (\Pi_{ij}(M_j^2) - \Pi_{ij}(0))/M_j^2$ (except $F_{\gamma\gamma} = \Pi_{\gamma\gamma}(M_Z^2)/M_Z^2$). These parameters can only be extracted from the data when M_H is fixed to a reference value. The following approximate formulas reproduce S, T and U within ± 0.01 for 60 GeV $< M_H <$ 1000 GeV:

$$\begin{aligned}
S &= -0.12 \pm 0.14 + 0.04(\tfrac{100\ \rm GeV}{M_H} - 1) - 0.13\log_{10}\tfrac{M_H}{100\ \rm GeV}, \\
T &= -0.10 \pm 0.14 + 0.08(\tfrac{100\ \rm GeV}{M_H} - 1) + 0.31\log_{10}\tfrac{M_H}{100\ \rm GeV}, \\
U &= +0.20 \pm 0.24 - 0.02(\tfrac{100\ \rm GeV}{M_H} - 1).
\end{aligned} \tag{3}$$

We see that all 3 oblique parameters are consistent with zero within 1σ. Now consider the supersymmetric contributions to S, T and U. Supersymmetry contributes to the S parameter with either sign, but that changes the overall χ^2 only by relatively small amounts typically of $\mathcal{O}(1)$. Contributions to T and U are positive definite, but U is increased by less than 0.1, which is much less than the present uncertainty. On the other hand, contributions to T can be significant, and since positive, Eq. (3) shows that strong constraints can be expected to be associated with T.

The general oblique fit in Eqs. (3) is not very suitable for supersymmetry. It is more appropriate to impose the constraints $T > 0$, $U > 0$, and 60 GeV $< M_H <$ 150 GeV, and to

[11] We use the definitions from reference [59], but redefine them to include only the contributions from new physics [60].

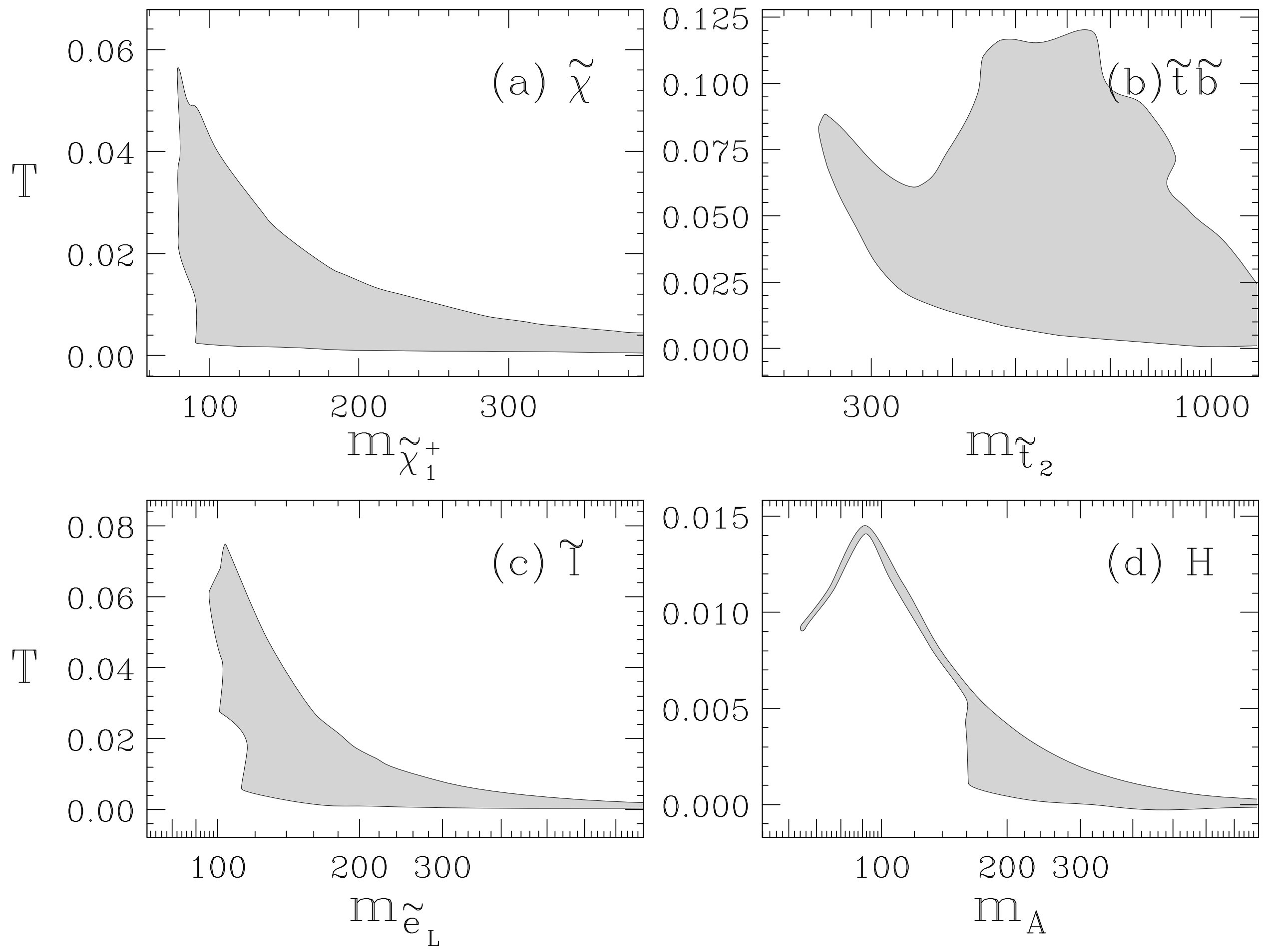

Figure 1: Supersymmetric contributions to the T parameter in the minimal supergravity model. Shown are (a) the chargino/neutralino contributions vs. the light chargino mass; (b) the stop/sbottom contributions vs. the heavy stop mass; (c) the slepton contributions vs. the left-handed selectron mass; and (d) the Higgs sector contributions vs. the CP–odd Higgs boson mass. Masses are in GeV.

deviate from the oblique approximation in allowing an extra parameter, γ_b, defined through [61] $\Gamma(Z \to b\bar{b}) = \Gamma^0(Z \to b\bar{b})(1+\gamma_b)$, in order to account for the possibility of supersymmetric $Zb\bar{b}$ vertex corrections. The result is[12]

$$\begin{aligned} S &= -0.09^{+0.18}_{-0.10}, \\ T &\leq +0.06, \\ U &= +0.17^{+0.23}_{-0.17}, \\ \gamma_b &= 0.006 \pm 0.004. \end{aligned} \tag{4}$$

If we redo this fit with $\gamma_b = 0$, the strong constraint, $T \leq 0.06$ is relaxed to $T \lesssim 0.08$. Eq. (4) shows that the T parameter is the most important of the three oblique parameters in determining the goodness of the fit. We show the various supersymmetric contributions to the T parameter in Fig. 1 in the supergravity model. The shaded regions are determined by

[12]This fit does not include the constraint from $B(B \to X_s\gamma)$.

randomly choosing $\mathcal{O}(10^5)$ points in parameter space (1) to find 50,000 quaint points. We see that the maximal contributions from each of the three superpartner sectors, gauginos, third generation squarks, and sleptons are significant ($\delta T_{\rm max} \sim 0.06$, 0.12, and 0.08, respectively). The Higgs sector[13] (and the first two generations of squarks) contributes at a lower level ($\delta T_{\rm max} \sim 0.015$). This pattern holds for the S and U parameters as well.

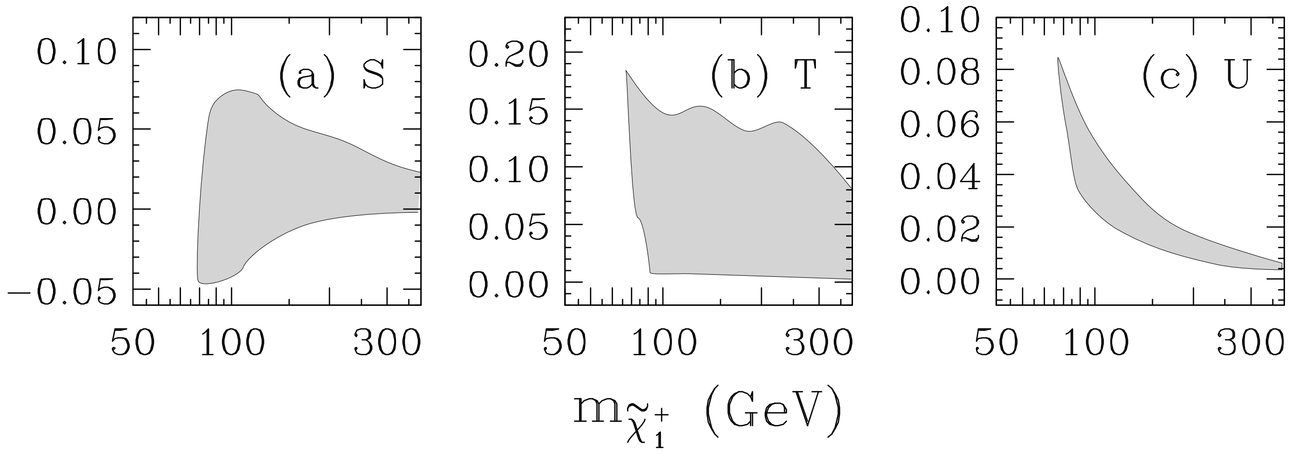

Figure 2: Supersymmetric contributions to the S, T, and U parameters vs. the light chargino mass, in the supergravity model.

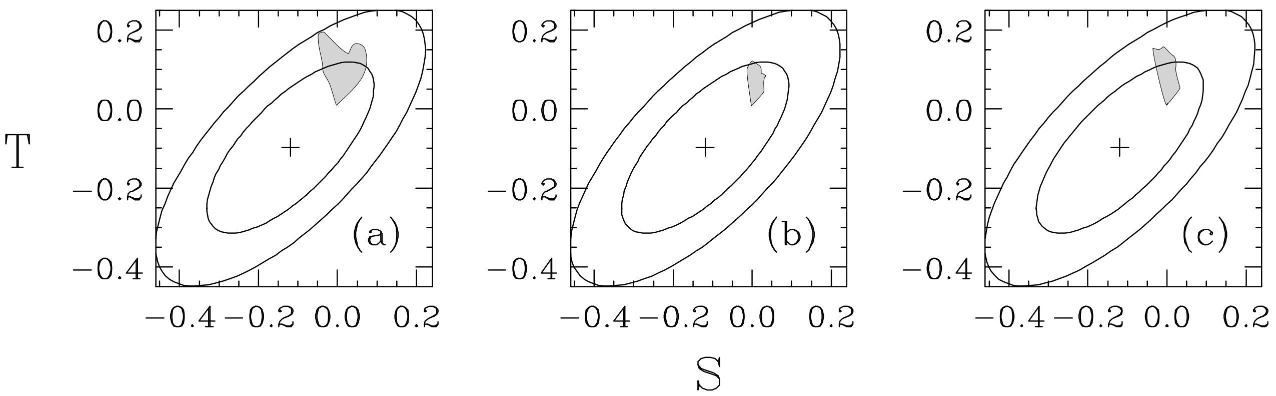

Figure 3: Supersymmetric contributions to the S and T parameters. Shown are the results for (a) the minimal supergravity model; (b) the $\mathbf{5}+\overline{\mathbf{5}}$ gauge-mediated model; and (c) the $\mathbf{10}+\overline{\mathbf{10}}$ gauge-mediated model. The best fit value (+) and 68 and 95% CL contours of S and T are also shown, for $M_H = 100$ GeV. Note that by definition $S = T = 0$ in the SM.

We show the total contribution from all superpartners and extra Higgs bosons to S, T and U in Fig. 2. Here we see that these contributions are approximately in the range (−0.05

[13]The Higgs sector contribution is evaluated by computing the MSSM Higgs sector contribution and subtracting the SM Higgs sector contribution, with the SM Higgs boson mass equal to the light MSSM Higgs boson mass.

to +0.08), (0 to 0.2), and (0 to 0.09), respectively, for S, T and U, and the decoupling of supersymmetry from these parameters is evident. These contributions are significantly limited by the recent, more stringent collider bounds on new particle masses discussed above. In the gauge-mediated models, the maximum contribution to the oblique parameters is even further reduced. We illustrate this in Fig. 3, which shows the allowed regions in the S–T plane for the three models. We also show the best fit values of S and T, and the 68% and 95% contours, determined with M_H fixed at 100 GeV. It is important to realize that the difference in χ^2 between the SM minimum and the minimum allowing freely varying oblique parameters is only one unit. Hence, even with the best possible addition of oblique corrections, the χ^2 will not improve significantly with respect to the SM. Moreover, Fig. 3 nicely illustrates two points. First, the corrections from supersymmetry are quite limited in magnitude, and second, they tend to worsen the fit compared to the SM.

Judging from Fig. 3, it appears that no or very little of the supersymmetric parameter space can be excluded. However, the oblique approximation is just that, an approximation. As we will show, it cannot be used to reliably indicate whether parameter space is excluded. The oblique approximation neglects higher order terms in the derivative expansion, as well as the non-universal corrections: the vertex corrections, wave-function renormalization, and box diagrams. We illustrate the relative magnitude of the oblique and non-oblique corrections to many of the observables in Fig. 4, in the supergravity model. Here, we show the full range of the shifts of each observable due to the shift in each oblique parameter[14], labeled `S, T, U`, and their sum[15], labeled `obl`. For comparison, just below the range of the shift from the total oblique correction we indicate the non-oblique corrections at the endpoints of that range. Therefore one can compare the oblique and non-oblique corrections at the points of maximal positive and negative oblique shift. We also show the range of the non-oblique corrections in our scan, labeled `n-obl`, and just below that, for comparison, the corresponding oblique correction at the points of maximal positive and negative non-oblique shift. Finally, we show the range of the full one-loop corrections, labeled `full`, and at the points of maximal positive and negative full correction we indicate the relative sizes of the oblique and non-oblique parts. All these shifts are shown in units of standard deviation, i.e. we divide each shift by the experimental error. The APV observables, the neutrino scattering observables, as well as $A_{LR}^{FB}(\mu)$, $A_{LR}^{FB}(b)$, $A_{LR}^{FB}(c)$, and R_c, all receive very small shifts, and are not shown. We show the same plots for the $\mathbf{5}+\overline{\mathbf{5}}$ and $\mathbf{10}+\overline{\mathbf{10}}$ gauge mediation models in Figs. 5 and 6. From these figures we see that, in all three models, the non-oblique corrections can be larger than the oblique corrections *for every observable except* M_W (and Γ_Z in the supergravity model). Hence it is essential to include the full corrections in this type of analysis.

Figs. 4–6 also show that the largest corrections occur in the supergravity model, and the smallest in the $\mathbf{5}+\overline{\mathbf{5}}$ gauge-mediated model. In each model the gaugino masses obey the usual GUT relation, i.e. $M_i \propto \alpha_i$. For a given gaugino mass scale, the scalar spectra (and the Higgsino mass) in the three models vary. The model with the lightest scalars (for a fixed

[14]Only M_W receives non-negligible contributions from the U parameter. In particular, the DIS variable κ is insensitive to U, although DIS results are frequently quoted in terms of $\sin^2\theta_W = 1 - M_W^2/M_Z^2$. Clearly, in the presence of new physics such quotes can be misleading.

[15]The shift from the maximal total oblique correction is not necessarily the sum of the shifts due to the individual maximal oblique corrections, because the individual corrections need not find their maximal values at the same point in parameter space.

gaugino mass) is the supergravity model, in the region $M_0 \ll M_{1/2}$. It is in this region (actually $M_0 \sim M_{1/2}/2$) that the largest corrections occur. The $\mathbf{5}+\overline{\mathbf{5}}$ gauge-mediated model has the heaviest scalar spectrum, and hence the smallest corrections (Fig. 5). The ratio of scalar mass to gaugino mass is proportional to $1/\sqrt{n_5^{\rm eff}}$, where $n_5^{\rm eff}$ is the effective number of $\mathbf{5}+\overline{\mathbf{5}}$ pairs. Hence, the scalar masses can be made relatively lighter in the gauge-mediated case if $n_5^{\rm eff}$ is increased. The $\mathbf{10}+\overline{\mathbf{10}}$ model we consider corresponds to $n_5^{\rm eff}=3$, and the relatively lighter scalars give rise to larger corrections (Fig. 6). However, they are still not as large as in the supergravity model. We expect the magnitude of the corrections in the case[16] $n_5^{\rm eff}=4$ to match quite closely with the supergravity results, as in this case the two spectra can have significant overlap (see Figure 10, Table 1, and the corresponding discussion in Ref. [62], for an example). Figs. 5 and 6 show that insensitive observables in the supergravity model are likewise insensitive in the $\mathbf{5}+\overline{\mathbf{5}}$ and $\mathbf{10}+\overline{\mathbf{10}}$ gauge mediation models.

Figure 7 shows, for each model, the range of the best fit predictions of each observable found in our scan over quaint parameter space, in units of standard deviation. We also indicate the best fit value of each observable in the SM. Note that the range of each observable in the supersymmetric models always includes the SM best fit value, since the supersymmetric corrections decouple, and the range of the supersymmetric light Higgs boson mass includes the best fit SM Higgs mass. The best fit values of the observables which are most sensitive to supersymmetric contributions, Γ_Z, $A^{FB}(b)$, and the SLC measurement of A_e, can vary over a range of $\sim 1\sigma$. This range for the best fit predictions is smaller than the actual contributions from supersymmetry shown in Figs. 4–6, which can be larger than 2σ. This is because the standard parameters adjust themselves to minimize the overall χ^2. The sensitivity of Γ_Z, $A^{FB}(b)$, and A_e are due to the very high precision with which these observables are measured. Shifts in M_W are somewhat smaller, but still important. Taken together, these large shifts do not improve but rather worsen the fit. They give rise to regions in parameter space which can be excluded. We describe these excluded regions in the next section. Not shown in Fig. 7 are correlations among the supersymmetric corrections. These correlations figure importantly in the fit. For example, in the region of parameter space where the supersymmetric prediction for R_b is closest to the measured value, the discrepancy in $A^{FB}(b)$ is much worse.

4 Results

The allowed and excluded quaint regions in a variety of two-dimensional parameter subspaces are shown in Figs. 8 and 9 for $\mu < 0$, and in Figs. 10, 11, and 12 for $\mu > 0$. These plots are the main result of our analysis. Each row of these figures shows the results for the supergravity model, the $\mathbf{5}+\overline{\mathbf{5}}$ gauge-mediated model, and the $\mathbf{10}+\overline{\mathbf{10}}$ gauge-mediated model, respectively from left to right. We show with a solid line the region of parameter space where it is possible to find $\Delta\chi^2 < 3.84$. With a dashed line we indicate the region where it is possible to find $\Delta\chi^2 > 3.84$. Hence, those regions enclosed by a dashed line but not by a solid line are excluded, independently of the value of any other parameter. Of course, in the regions bounded by a dashed line *and* a solid line there are both allowed and excluded points. In some cases we plot the shift δ from supersymmetry rather than the value of the observable. We show more results in the $\mu > 0$ case because of the larger excluded region, as discussed

[16]This corresponds to an SO(10) model with a $\mathbf{16}+\overline{\mathbf{16}}$ pair of fields.

below. In the following discussion, we use the abbreviations SUGRA, GM_5, and GM_{10} to refer to the minimal supergravity, $\mathbf{5}+\overline{\mathbf{5}}$ and $\mathbf{10}+\overline{\mathbf{10}}$ gauge-mediated models. Also, GM refers to *both* the $\mathbf{5}+\overline{\mathbf{5}}$ and $\mathbf{10}+\overline{\mathbf{10}}$ models, and limits listed as three consecutive numbers refer to the SUGRA, GM_5, and GM_{10} models, respectively.

Figs. 8 (a–c) and 10 (j–l) demonstrate the importance of the $B(B \to X_s\gamma)$ observable for our results[17]. When included much larger values of $\Delta\chi^2$ are possible. Large parts of parameter space are excluded due to unacceptably large positive or negative contributions to the $b \to s\gamma$ amplitude, especially with $\mu > 0$. The most important corrections are due to chargino/top-squark loops. These contributions are proportional to $\mu \tan\beta$, at large $\tan\beta$. Hence, for $\mu > 0$, they constructively add to the SM and charged Higgs amplitudes, and very large total amplitudes can result over a wide region of parameter space. For large negative μ, the chargino amplitude destructively interferes with the SM and charged Higgs amplitudes, and the full one-loop amplitude can vanish. However, this cancellation occurs only in a relatively small region of parameter space. Either case can result in a very large contribution to $\Delta\chi^2$. Because of the strong impact of this observable we have chosen a more conservative error assignment for it (see Section 2).

As a first example of how the $\mu > 0$ region of parameter space is more severely constrained than the $\mu < 0$ region, consider the input parameters in the supergravity model. In the $\mu > 0$ case, the no-scale model [66] (i.e. $M_0 = 0$) is seen to be excluded[18]. Specifically, we find the independent limits $M_0 \geq 9$ GeV and $M_{1/2} \gtrsim 105$ GeV (Fig. 10(a)). In the $\mu < 0$ case, by contrast, no limit on M_0 can be set, and the limit, $M_{1/2} \gtrsim 120$ GeV, is not improved by our analysis.

We should stress at this point that, for either sign of μ, there is some parameter space excluded even at the very largest values of M_0 and $M_{1/2}$ that we consider (1 and 0.5 TeV, respectively). Here we emphasize the bounds that are valid independently of the values of any other parameters. This is what we mean by "excluded regions". For emphasis we sometimes refer to these regions as "absolutely excluded".

The input parameter which sets the scale of the superpartner spectrum in the gauge-mediated models, Λ, is constrained in the $\mu > 0$ case to be larger than 36 (14) TeV in the GM_5 (GM_{10}) model, whereas the entire (quaint) parameter space extends down to 28 (10) TeV (Figs. 10 (b–c)). Again, the corresponding bound with $\mu < 0$ of 41 (13) TeV could not be improved significantly.

Similarly, Figs. 11 (d–f) show that for $\mu > 0$, $\tan\beta < 36$, 45 and 39, respectively, for the three models. In contrast, for $\mu < 0$ values of $\tan\beta$ as large as 65 are still allowed.

Figs. 10 (d–f) illustrate how the oblique parameters can serve as useful barometers in parametrizing the excluded region of supersymmetric parameter space. Here we see, for $\mu > 0$, the allowed and excluded regions in the S–T plane. The region with $T \geq 0.12$ (0.07) is excluded

[17]Since the next-to-leading order calculation of $B(B \to X_s\gamma)$ is not available in the MSSM, we use an improved leading order formula in the Standard Model calculation [63], and include the leading order supersymmetric corrections [64]. With $\alpha_s = 0.118$, $m_t = 175$ GeV, $m_b^{\rm pole} = 4.9$ GeV, $m_c/m_b = 0.3$ and the renormalization scale equal to m_b, our SM result for $B(B \to X_s\gamma)$, 3.36×10^{-4}, agrees with the result of the next-to-leading SM calculation given in Ref. [65], $(3.38 \pm 0.33) \times 10^{-4}$.

[18]Interesting bounds on M_0 and other supersymmetry parameters have also been obtained by studying charge and color breaking minima of the effective potential [67]. However, these bounds are relaxed when one considers the possibility that the tunneling time from a false to the true vacuum can exceed the lifetime of the universe [68].

in the SUGRA (GM) model. Also, we can read off positive and negative bounds on S.

The sensitivity of some of the observables is shown in Figs. 8 (a–c) and 10 (g–l). Here we see, for example, $\delta \sin^2 \theta^e_{\rm eff} \leq -6 \times 10^{-4}$ (-4×10^{-4}) and $\delta A^{FB}(b) \geq 4 \times 10^{-3}$ (3×10^{-3}) are excluded in the SUGRA (GM) model with $\mu > 0$.

The global precision analysis leads to interesting bounds on the superpartner and Higgs boson masses. In Fig. 11 (a–c) we show the significantly improved limits, $m_A > 320,\ 255,\ 230$ GeV, in the three models, with $\mu > 0$. In the $\mu < 0$ case these bounds are weakened to $m_A > 115$, 220, and 185 GeV (Figs. 8 (d–f)). These limits imply bounds on other Higgs boson masses. For example, the region with the lightest possible Higgs boson mass, $62.5 < m_h < 71$ GeV, is absolutely excluded, in every model and for any sgn(μ)[19]. The upper bound on m_h depends on the cut-off chosen for the squark mass scale. With an $\mathcal{O}(1)$ TeV cut-off the upper limit in the GM models, $m_h \lesssim 115$ GeV, is stronger by about 10 GeV compared to SUGRA due to the relative absence of mixing in the top squark sector. All the Higgs-boson mass lower limits primarily result from the $B(B \to X_s \gamma)$ constraint on the charged Higgs mass, e.g. $m_{H^+} > 330,\ 265,\ 240$ GeV, in the $\mu > 0$ case (Figs. 11 (d–f)).

The lower bounds on the lightest chargino mass, $m_{\tilde{\chi}_1^+} > 89,\ 100,\ 120$ GeV, are seen in Figs. 11 (g–i) in the $\mu > 0$ case, together with the corresponding bounds on the lightest neutralino mass. The indirect bounds on the squark (specifically $\tilde{u}_L$) and gluino masses can be read off of Figs. 11 (j–l) and 8 (g–i), and in the $\mu > 0$ case extend well beyond the direct limits. For example, the left-handed up-squark mass is bounded by 285 (355) GeV in the SUGRA (GM) model.

Both the direct and indirect limits on the third generation squark masses are different from the first two generations. The indirect bounds are illustrated in Figs. 9 (a–f) and 12 (a–f). For a large range of third generation squark masses, in some cases exceeding 1 TeV, it is possible to find excluded parameter space. However, the regions that are absolutely excluded are not so significant for these masses. In particular, the light top squark cannot be excluded in the SUGRA model (Fig. 12(d)). However, the heavy (predominantly left-handed) top squark mass is significantly bounded by $m_{\tilde{t}_2} \gtrsim 275$ (355) GeV in the SUGRA (GM) model, with $\mu > 0$.

The constraints on the slepton masses are shown in Figs. 12 (g–l) and, for the third generation, in Figs. 9 (g–i). The absolutely excluded bounds for these and other particle masses and model parameters are listed in Table 3. They combine our present knowledge from phenomenological constraints[20], direct searches and precision experiments. Entries marked by an asterisk are determined by the phenomenological constraints or the direct search limits, i.e. our global precision analysis does not improve the bound.

The range of best fit values of m_t is confined to the range 168–174 GeV in the parameter space with $\Delta\chi^2 < 3.84$. Thus, supersymmetry prefers m_t in the lower part of the allowed Tevatron range. The Z lineshape determination of α_s is known to be very sensitive to new physics, which in general alters the theoretical prediction for R_ℓ. This happens typically through vertex corrections or other corrections to the weak mixing angle. Our analysis reveals, however, that in the allowed regions of the investigated models, the fitted α_s values are within the small range 0.1195 ± 0.0006. Therefore, in the context of minimal gauge- or gravity-

[19] Table 3 reflects a stronger statement of this bound based on more recent LEP results, as discussed in the next section.

[20] We refer to electroweak symmetry breaking and Yukawa coupling perturbativity constraints.

mediated supersymmetry breaking (including the external constraint 0.118 ± 0.003),

$$\alpha_s = 0.1195 \pm 0.0022 \pm 0.0006,$$

where the first error is experimental and the second theoretical, i.e. from varying the supersymmetry parameters.

5 Conclusions and Outlook

Precision data continues to play an important role in discriminating and constraining various extensions of the standard model. For example, it is well known that the precision data analysis leads to serious constraints on technicolor models. Supersymmetric models can always avoid such constraints because the supersymmetric corrections decouple, so the supersymmetric models look just like the standard model if the supersymmetric mass scale is large enough (~ 0.5 to 1 TeV). As long as the standard model with a light Higgs boson provides a good fit to the data (the current fit is excellent), supersymmetric models can as well.

On the other hand, what if one were to consider a supersymmetric spectrum which includes light ($\mathcal{O}(M_Z)$) superpartners? Then it is interesting to investigate whether the global fits to the data become better or worse as a result of non-negligible supersymmetric corrections. This has been the purpose of this paper. To this end, we combined a state of the art standard model calculation with the one-loop supersymmetric corrections, and performed global fits to the precision observables in three supersymmetric models. We have shown that our global analysis leads (in many cases) to significantly improved bounds on the parameters and masses of the various models. For example, we have shown that for a positive μ-parameter the CP–odd Higgs boson mass lower bound increases from ~ 60 GeV to over 320 (230) GeV in the supergravity (gauge-mediated) model. For $\mu < 0$ the m_A bound is not as strong, but we are able to set a bound,

$$m_A > 115 \text{ GeV}, \tag{5}$$

for all models under consideration. This has an important consequence: as shown in Figure 21 of the very recent Ref. [40], there is unexcluded parameter space with $60 < m_h < 78$ GeV when $68 < m_A < 102$ GeV. With our bound (5) this part of parameter space is excluded and we conclude,

$$m_h \geq 78 \text{ GeV}, \tag{6}$$

i.e. the MSSM Higgs bound coincides with the SM one. The m_h bound (6) supersedes the bound of 71 GeV mentioned in Section 4, which has a similar origin, but was based on the data presented at the summer conferences [50]; for similar bounds with fixed values of $\tan\beta$ see Ref. [11].

We set many other interesting bounds, and our main results can be found in Table 3 and Figures 8–12. We advocate Table 3 as a reference for the current collider and precision bounds in an important class of supersymmetry breaking scenarios.

In summary, significant portions of the parameter spaces of popular supersymmetry breaking scenarios have been shown to be excluded, in particular, for $\mu > 0$. This has immediate consequences for the near future of collider experiments. LEP 2 will ultimately be able to discover a chargino with a mass up to about 100 GeV. Hence, LEP 2 is very unlikely to discover the chargino in the gauge mediation models with $\mu > 0$. The main injector at Fermilab, a possible further luminosity upgrade (TEV 33), and the LHC, however, will be able to cover a large part of parameter space which is not excluded by either present direct limits or precision experiments.

Note added: After submission of this paper there appeared an e-print [69] announcing new versions of the electroweak libraries ZFITTER and TOPAZ0. Their Standard Model predictions for electroweak observables are now very close to ours.

Acknowledgements

We would like to thank Paul Langacker for many valuable comments and suggestions. We thank Howard Haber, Peter Rowson, and Jim Wells for useful conversations. We greatly appreciate the hospitality and stimulating atmosphere of the Aspen Center for Physics and the CERN theory group. We are thankful for the hospitality of the University of Washington nuclear and particle theory groups, and thank the computing center staff at CERN and the University of Washington for support. We greatly benefitted from the one-loop integral package, `FF`, written by G.J. van Oldenborgh [70].

References

[1] E. Witten, *Nucl. Phys.* **B443**, 85 (1995).

[2] S. Dimopoulos, S. Raby, and F. Wilczek, *Phys. Rev.* **D24**, 1681 (1981);
L.E. Ibáñez and G.G. Ross, *Phys. Lett.* **105B**, 439 (1981);
U. Amaldi *et al.*, *Phys. Rev.* **D36**, 1385 (1987);
J. Ellis, S. Kelley, and D.V. Nanopoulos, *Phys. Lett.* **249B**, 441 (1990);
P. Langacker and M.-X. Luo, *Phys. Rev.* **D44**, 817 (1991);
U. Amaldi, W. de Boer, and H. Fürstenau, *Phys. Lett.* **260B**, 447 (1991);
P. Langacker and N. Polonsky, *Phys. Rev.* **D47**, 4028 (1993) and *ibid.* **D52**, 3081 (1995);
P.H. Chankowski, Z. Płuciennik, and S. Pokorski, *Nucl. Phys.* **B439**, 23 (1995);
J. Bagger, K. Matchev, and D. Pierce, *Phys. Lett.* **348B**, 443 (1995).

[3] See H.P. Nilles, *Phys. Rep.* **110**, 1 (1984) for a review and references.

[4] H.P. Nilles, *Nucl. Phys.* **B217**, 366 (1983).

[5] H.P. Nilles, *Phys. Lett.* **115B**, 193 (1982) and *Nucl. Phys.* **B217**, 366 (1983);
S. Ferrara, L. Girardello, and H.P. Nilles, *Phys. Lett.* **125B**, 457 (1983).

[6] M. Dine, W. Fischler, and M. Srednicki, *Nucl. Phys.* **B189**, 575 (1981);
S. Dimopoulos and S. Raby, *Nucl. Phys.* **B192**, 353 (1981);
M. Dine and M. Srednicki, *Nucl. Phys.* **B202**, 238 (1982);

L. Alvarez-Gaumé, M. Claudson, and M.B. Wise, *Nucl. Phys.* **B207**, 96 (1982);
C.R. Nappi and B.A. Ovrut, *Phys. Lett.* **113B**, 175 (1982);
I. Affleck, M. Dine, and N. Seiberg, *Nucl. Phys.* **B256**, 557 (1985);
M. Dine and W. Fischler, *Phys. Lett.* **110B**, 227 (1992);
M. Dine and A.E. Nelson, *Phys. Rev.* **D48**, 1277 (1993);
J. Bagger, E. Poppitz, and L. Randall, *Nucl. Phys.* **B426**, 3 (1994);
M. Dine, A.E. Nelson, and Y. Shirman, *Phys. Rev.* **D51**, 1362 (1995).

[7] D. Garcia and J. Solà, *Phys. Lett.* **354B**, 335 (1995);
G.L. Kane, R.G. Stuart, and J.D. Wells, *Phys. Lett.* **354B**, 350 (1995);
P.H. Chankowski and S. Pokorski, *Phys. Lett.* **366B**, 188 (1996);
W. de Boer *et al.*, *Z. Phys.* **C75**, 627 (1997);
For other references discussing supersymmetry and precision observables, see [8, 9, 10, 11].

[8] D.M. Pierce and J. Erler, e-print `hep-ph/9708374`, talk presented at the 5th International Conference on Physics Beyond the Standard Model, Balholm (1997).

[9] M. Drees, K. Hagiwara, and A. Yamada, *Phys. Rev.* **D45**, 1725 (1992);
G. Altarelli, R. Barbieri, and F. Caravaglios, *Phys. Lett.* **314B**, 357 (1993);
D. Garcia and J. Solà, *Mod. Phys. Lett.* **A9**, 211 (1994);
D. Garcia, R.A. Jiménez and J. Solà, *Phys. Lett.* **347B**, 309 (1995), *ibid.* **347B**, 321 (1995), and Erratum *ibid.* **351B**, 602 (1995);
P.H. Chankowski, J. Ellis and S. Pokorski, e-print `hep-ph/9712234`;
P.H. Chankowski and S. Pokorski, e-print `hep-ph/9707497`, to appear in *Perspectives on Supersymmetry*, ed. G.L. Kane (World Scientific, Singapore);
W. Hollik, e-print `hep-ph/9711489`, talk given at the International Workshop on Quantum Effects in the MSSM, Barcelona (1997);
W. de Boer *et al.*, e-print `hep-ph/9712376`.

[10] D.M. Pierce, J.A. Bagger, K. Matchev, and R.-J. Zhang, *Nucl. Phys.* **B491**, 3 (1997).

[11] P.H. Chankowski, e-print `hep-ph/9711470`, in the proceedings of the International Workshop on Quantum Effects in the MSSM, Barcelona (1997).

[12] M.E. Peskin and T. Takeuchi, *Phys. Rev. Lett.* **65**, 964 (1990) and *Phys. Rev.* **D46**, 381 (1992).

[13] For more details and an extensive list of references to radiative corrections in the SM see J. Erler and P. Langacker, *Electroweak Model and Constraints on New Physics*, in Ref. [14].

[14] R.M. Barnett *et al.*, *Phys. Rev.* **D54**, 1 (1996) and 1997 off-year partial update for the 1998 edition available on the PDG WWW pages (URL: `http://pdg.lbl.gov/`).

[15] R. Harlander, T. Seidensticker, and M. Steinhauser, e-print `hep-ph/9712228`.

[16] The LEP Collaborations ALEPH, DELPHI, L3, OPAL, the LEP Electroweak Working Group, and the SLD Heavy Flavour Group: D. Abbaneo *et al.*, preprint LEPEWWG/97–02.

[17] SLD Collaboration: K. Abe *et al.*, *Phys. Rev. Lett.* **78**, 2075 (1997), and P.C. Rowson, talk presented at the 32nd Rencontres de Moriond: Electroweak Interactions and Unified Theories, Les Arcs (1997).

[18] SLD Collaboration: K. Abe *et al.*, *Phys. Rev. Lett.* **79**, 804 (1997).

[19] SLD Collaboration: K. Abe *et al.*, *Phys. Rev. Lett.* **78**, 17 (1997).

[20] CDF Collaboration: F. Abe *et al.*, *Phys. Rev. Lett.* **75**, 11 (1995), *Phys. Rev.* **D52**, 4784 (1995), and R.G. Wagner, talk presented at the 5th International Conference on Physics Beyond the Standard Model, Balholm (1997).

[21] DØ Collaboration: S. Abachi *et al.*, *Phys. Rev. Lett.* **77**, 3309 (1996), and B. Abbott *et al.*, preprint Fermilab–Conf–97–354–E, submitted to the XVIII International Symposium on Lepton Photon Interactions, Hamburg (1997).

[22] UA2 Collaboration: S. Alitti *et al.*, *Phys. Lett.* **276B**, 354 (1992).

[23] CDF Collaboration: F. Abe *et al.*, *Phys. Rev. Lett.* **79**, 1992 (1997), and S. Leone, talk presented at the High-Energy Physics International Euroconference on Quantum Chromodynamics (QCD 97), Montpellier (1997).

[24] DØ Collaboration: S. Abachi *et al.*, *Phys. Rev. Lett.* **79**, 1197 (1997), and B. Abbott *et al.*, e-print `hep-ex/9706014`.

[25] Oxford: N.H. Edwards, S.J. Phipp, P.E.G. Baird, and S. Nakayama, *Phys. Rev. Lett.* **74**, 2654 (1995).

[26] Seattle: P.A. Vetter, *et al.*, *Phys. Rev. Lett.* **74**, 2658 (1995).

[27] Boulder: C.S. Wood *et al.*, *Science* **275**, 1759 (1997).

[28] CCFR Collaboration: K.S. McFarland *et al.*, e-print `hep-ex/9701010`.

[29] CDHS Collaboration: H. Abramowicz *et al.*, *Phys. Rev. Lett.* **57**, 298 (1986), and A. Blondel *et al.*, *Z. Phys.* **C45**, 361 (1990).

[30] CHARM Collaboration: J.V. Allaby *et al.*, *Phys. Lett.* **117B**, 446 (1986) and *Z. Phys.* **C36**, 611 (1987).

[31] CHARM II Collaboration: P. Vilain *et al.*, *Phys. Lett.* **335B**, 246 (1994);
for earlier results see J. Panman, p. 504 of [32].

[32] *Precision Tests of the Standard Electroweak Model*, ed. P. Langacker (World Scientific, Singapore, 1995).

[33] CLEO Collaboration: M.S. Alam *et al.*, *Phys. Rev. Lett.* **74**, 2885 (1995).

[34] For a comprehensive introduction and review of applied statistics and data analysis see A. Gelman, J.B. Carlin, H.S. Stern, and D.B. Rubin, *Bayesian Data Analysis*, (Chapman & Hall, London, 1995).

[35] K. Adel and Y.P. Yao, *Phys. Rev.* **D49**, 4945 (1994);
A.J. Buras, M. Misiak, M. Münz, and S. Pokorski, *Nucl. Phys.* **B424**, 374 (1994);
A. Ali and C. Greub, *Phys. Lett.* **361B**, 146 (1995);
C. Greub, T. Hurth, and D. Wyler, *Phys. Lett.* **380B**, 385 (1996) and *Phys. Rev.* **D54**, 3350 (1996);
A.J. Buras, A. Kwiatkowski, and N. Pott, e-print `hep-ph/9707482`;
M. Ciuchini, G. Degrassi, P. Gambino, and G.F. Giudice, e-print `hep-ph/9710335`.

[36] R. Alemany, M. Davier, and A. Höcker, e-print `hep-ph/9703220`.

[37] For recent reviews see P. N. Burrows, *Acta Phys. Polon.* **B28**, 701 (1997), and
I. Hinchliffe, *Quantum Chromodynamics*, in Ref. [14].

[38] G. Degrassi, P. Gambino, and A. Vicini, *Phys. Lett.* **383B**, 219 (1996).

[39] A. Czarnecki and J.H. Kühn, *Phys. Rev. Lett.* **77**, 3955 (1996).

[40] A. Sopczak, e-print `hep-ph/9712283`, talk presented at the 1st International Workshop on Nonaccelerator New Physics (NANP 97), Dubna (1997).

[41] DELPHI Collaboration: P. Abreu *et al.*, *Z. Phys.* **C67**, 1 (1995), and E. Boudinov *et al.*, submitted to the International Europhysics Conference on High Energy Physics (HEP 97), Jerusalem (1997).

[42] J. Erler, *Phys. Rev.* **D52**, 28 (1995).

[43] J. Erler, J.L. Feng, and N. Polonsky, *Phys. Rev. Lett.* **78**, 3063 (1997).

[44] L. Girardello and M.T. Grisaru, *Nucl. Phys.* **B194**, 65 (1982);
H.P. Nilles, M. Srednicki, and D. Wyler, *Phys. Lett.* **120B**, 346 (1983).

[45] N. Polonsky and A. Pomarol, *Phys. Rev. Lett.* **73**, 2292 (1994) and *Phys. Rev.* **D51**, 6532 (1995).

[46] S. Dimopoulos and D. Sutter, *Nucl. Phys.* **B452**, 496 (1995);
S. Raby, *Phys. Rev.* **D56**, 2852 (1997).

[47] M. Dine, A.E. Nelson, Y. Nir, and Y. Shirman, *Phys. Rev.* **D53**, 2658 (1996);
G. Dvali, G.F. Giudice, and A. Pomarol, *Nucl. Phys.* **B478**, 31 (1996).

[48] J.A. Grifols and J. Solà, *Phys. Lett.* **137B**, 257 (1984) and *Nucl. Phys.* **B253**, 47 (1985);
P.H. Chankowski *et al.*, *Nucl. Phys.* **B417**, 101 (1994).

[49] A. Denner, R. Guth, W. Hollik, J.H. Kühn, *Z. Phys.* **C51**, 695 (1991);
M. Boulware and D. Finnell, *Phys. Rev.* **D44**, 2054 (1991);
J.D. Wells, C. Kolda and G.L. Kane, *Phys. Lett.* **338B**, 219 (1994);
M. Drees *et al.*, *Phys. Rev.* **D54**, 5598 (1996);
P.H. Chankowski and S. Pokorski, *Nucl. Phys.* **B475**, 3 (1996).

[50] ALEPH Collaboration: R. Barate *et al.*, report EPS–HEP97–748, to appear in the proceedings of the International Europhysics Conference on High Energy Physics (HEP 97), Jerusalem (1997).

[51] P. Janot, talk presented at the International Europhysics Conference on High Energy Physics (HEP 97), Jerusalem (1997).

[52] ALEPH Collaboration: R. Barate *et al.*, *Phys. Lett.* **407B**, 377 (1997).

[53] F. Cerutti, talk presented at the 5th International Conference on Supersymmetries in Physics (SUSY 97), Philadelphia (1997).

[54] DØ Collaboration: S. Abachi *et al.*, *Phys. Rev. Lett.* **76**, 2222 (1996).

[55] ALEPH Collaboration: R. Barate *et al.*, *Phys. Lett.* **405B**, 379 (1997).

[56] CDF Collaboration: F. Abe *et al.*, *Phys. Rev.* **D56**, 1357 (1997).

[57] T. Bayes, *Phil. Trans.* **53**, 370 (1763), reprinted in *Biometrica* **45**, 296 (1958).

[58] R. Barbieri and G.F. Giudice, *Nucl. Phys.* **B306**, 63 (1988);
G.W. Anderson and D.J. Castaño, *Phys. Lett.* **347B**, 300 (1995);
S. Dimopoulos and G.F. Giudice, *Phys. Lett.* **357B**, 573 (1995).

[59] W.J. Marciano and J.L. Rosner, *Phys. Rev. Lett.* **65**, 2963 (1990) and Erratum *ibid.* **68**, 898 (1992).

[60] J. Erler and P. Langacker, *Phys. Rev.* **D52**, 441 (1995).

[61] G. Altarelli, R. Barbieri, and F. Caravaglios, *Nucl. Phys.* **B405**, 3 (1993).

[62] J.A. Bagger, K. Matchev, D. M. Pierce, and R.J. Zhang, *Phys. Rev.* **D55**, 3188 (1997).

[63] P. Cho and B. Grinstein, *Nucl. Phys.* **B365**, 279 (1991) and Erratum *ibid.* **B427**, 697 (1994).

[64] S. Bertolini, F. Borzumati, A. Masiero, G. Ridolfi, *Nucl. Phys.* **B353**, 591 (1991);
R. Barbieri, G.F. Giudice, *Phys. Lett.* **309B**, 86 (1993);
J.L. Hewett and J.D. Wells, *Phys. Rev.* **D55**, 5549 (1997);
H. Baer and M. Brhlik, *Phys. Rev.* **D55**, 3201 (1997).

[65] K. Chetyrkin, M. Misiak, and M. Münz, *Phys. Lett.* **400B**, 206 (1997);
C. Greub and T. Hurth, *Phys. Rev.* **D56**, 2934 (1997).

[66] A.B. Lahanas and D.V. Nanopoulos, *Phys. Rep.* **145**, 1 (1987).

[67] J.A. Casas, A. Lleyda, and C. Muñoz, *Phys. Lett.* **389B**, 305 (1996).

[68] A. Kusenko, P. Langacker, and G. Segre, *Phys. Rev.* **D54**, 5824 (1996);
A. Kusenko and P. Langacker, *Phys. Lett.* **391B**, 29 (1997).

[69] D. Bardin and G. Passarino, e-print `hep-ph/9803425`.

[70] G.J. van Oldenborgh and J.A.M. Vermaseren, *Z. Phys.* **C46**, 425 (1990); G.J. van Oldenborgh, *Comput. Phys. Commun* **66**, 1 (1991).

	measurement	SM	pull
M_Z [GeV]	91.1867 ± 0.0020	91.1867	0.0
Γ_Z [GeV]	2.4948 ± 0.0025	2.4959	-0.4
$\sigma_{\rm had}$[nb]	41.486 ± 0.053	41.478	0.2
R_e	20.757 ± 0.056	20.744	0.2
R_μ	20.783 ± 0.037	20.744	1.1
R_τ	20.823 ± 0.050	20.789	0.7
$A^{FB}(e)$	0.0160 ± 0.0024	0.0163	-0.1
$A^{FB}(\mu)$	0.0163 ± 0.0014	0.0163	0.0
$A^{FB}(\tau)$	0.0192 ± 0.0018	0.0163	1.6
$\mathcal{P}(\tau)$	0.1411 ± 0.0064	0.1476	-1.0
$\mathcal{P}^{FB}(\tau)$	0.1399 ± 0.0073	0.1476	-1.1
$\sin^2\theta^e_{\rm eff}(Q^{FB})$	0.2322 ± 0.0010	0.2315	0.8
R_b	0.2170 ± 0.0009	0.2158	1.3
R_c	0.1734 ± 0.0048	0.1722	0.2
$A^{FB}(b)$	0.0984 ± 0.0024	0.1035	-2.1
$A^{FB}(c)$	0.0741 ± 0.0048	0.0739	0.0
$A^{FB}_{LR}(b)$	0.900 ± 0.050	0.935	-0.7
$A^{FB}_{LR}(c)$	0.650 ± 0.058	0.668	-0.3
A_e	0.1548 ± 0.0033	0.1476	2.2
$A^{FB}_{LR}(\mu)$	0.102 ± 0.034	0.148	-1.3
$A^{FB}_{LR}(\tau)$	0.195 ± 0.034	0.148	1.4
M_W [GeV]	80.430 ± 0.076	80.386	0.6
m_t [GeV]	175 ± 5	172	0.6
Q_W(Cs)	-72.11 ± 0.93	-73.11	1.1
Q_W(Tl)	-114.8 ± 3.7	-116.7	0.5
κ(DIS)	0.581 ± 0.0039	0.583	-0.7
$g_V^{\nu e}$	-0.041 ± 0.015	-0.0396	-0.1
$g_A^{\nu e}$	-0.507 ± 0.014	-0.5064	0.0
$\lg(B(B \to X_s\gamma))$	-8.49 ± 0.45	-7.99	-1.1
$\Delta\alpha^{(5)}_{\rm had}$	0.02817 ± 0.00062	0.02817	0.0
$\alpha_s(M_Z)$	0.118 ± 0.003	0.1195	-0.5

Table 2: Results of a global fit to the Standard Model. For each observable, we list the experimental result, the best fit result within the SM with the Higgs mass allowed as a free parameter, and the pull.

model		SUGRA		GM$_5$		GM$_{10}$	
sgn (μ)		$+$	$-$	$+$	$-$	$+$	$-$
M_0		9	0*	—	—	—	—
$M_{1/2}$		105	120	—	—	—	—
Λ		—	—	36	41	14	13*
$\|\mu\|$		135*	135*	200	200	180	165
$\tan\beta$	$>$	1.4*	1.2*	1.3*	1.2*	1.3*	1.2*
$\tan\beta$	$<$	36	60*	45	65*	39	52*
m_h		78	78*	78	78*	78	78*
m_H		320	115	255	220	230	185
m_A		320	115	255	220	230	185
m_{H+}		330	140	265	235	240	205
$m_{\tilde{\chi}_1^0}$		45	46	51	50*	61	48*
$m_{\tilde{\chi}_2^0}$		89	83	100	91*	120	85*
$m_{\tilde{\chi}_3^0}$		150*	150*	215	210	190	175
$m_{\tilde{\chi}_4^0}$		195	205*	230	235	225	215
$m_{\tilde{\chi}_1^+}$		90	80	100	89*	120	82*
$m_{\tilde{\chi}_2^+}$		195	205*	235	240	230	220
$m_{\tilde{g}}$		255	285	285	320*	350	335*
$m_{\tilde{e}_R}$		74	66*	73	76*	70	63*
$m_{\tilde{e}_L}$		105	110	140	150	125	120
$m_{\tilde{\tau}_1}$		53	48*	73	55	70	52
$m_{\tilde{\tau}_2}$		110	110	140	150	125	120
$m_{\tilde{u}_L}$		285	295	355	405*	355	335*
$m_{\tilde{u}_R}$		280	290	330	375*	340	325*
$m_{\tilde{d}_L}$		295	305	360	410*	360	345*
$m_{\tilde{d}_R}$		285	290	325	370*	335	325*
$m_{\tilde{t}_1}$		56	66	275	170*	290	175*
$m_{\tilde{t}_2}$		275	310	355	420	365	385
$m_{\tilde{b}_1}$		185	250	320	345	330	310
$m_{\tilde{b}_2}$		285	295	325	370*	335	330*
S	$>$	-0.02	-0.02	0.00	0.00*	-0.01	0.00
S	$<$	$+0.04$	$+0.07$*	$+0.01$	$+0.03$	0.00	$+0.03$*
T	$<$	0.12	0.15	0.07	0.08	0.07	0.12*
U	$<$	0.03	0.05	0.02	0.03	0.02	0.05*

Table 3: Limits on model parameters and superpartner and Higgs-boson masses. All masses and mass parameters are in GeV (except for Λ in TeV) and are lower limits. Limits for S, T, U, and $\tan\beta$ are as indicated (T and U are positive definite). Entries marked by an asterisk are consequences of constraints from electroweak symmetry breaking, Yukawa perturbativity, or direct searches, and are not significantly improved by our analysis.

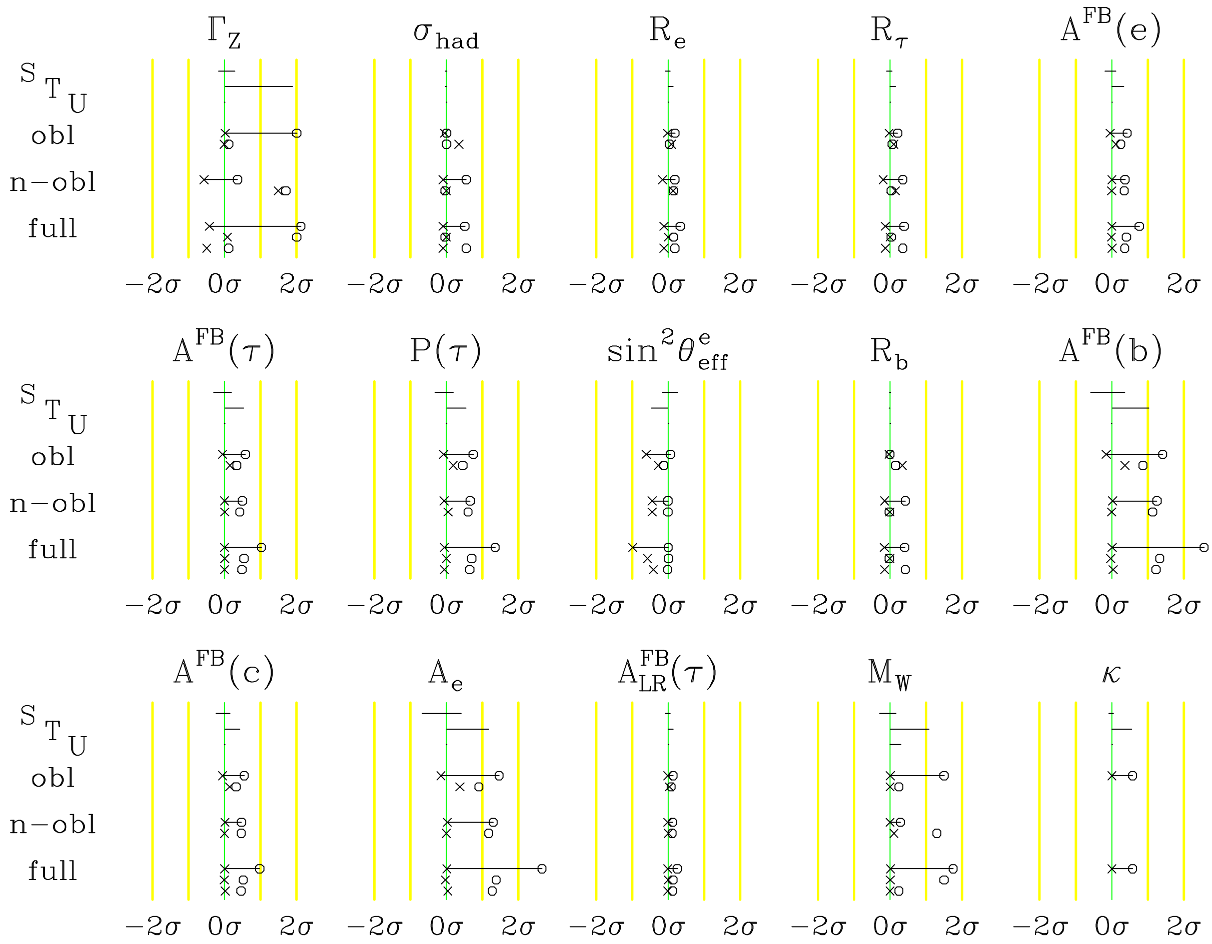

Figure 4: Supersymmetric contributions to various precision observables in the supergravity model. Shown is the effect on each observable (in units of standard deviation) when each oblique parameter, S, T, or U, is varied within its possible range in the supergravity model. Similarly, we show the full range of the combined effect of all three oblique parameters (labeled `obl`), so that a circle (cross) corresponds to the point with the largest positive (negative) oblique shift for that observable. Just below, we indicate the size of the corresponding non-oblique corrections at these points. Likewise, the full range of the non-oblique corrections are shown (labeled `n-obl`), and just below the corresponding oblique corrections at the extrema of this range are indicated. Finally, we show the range of the full corrections found in our scan (labeled `full`), and at the endpoints of this range we break the corrections down into their oblique and non-oblique parts. These are indicated just below, respectively. The non-oblique corrections to κ are not shown.

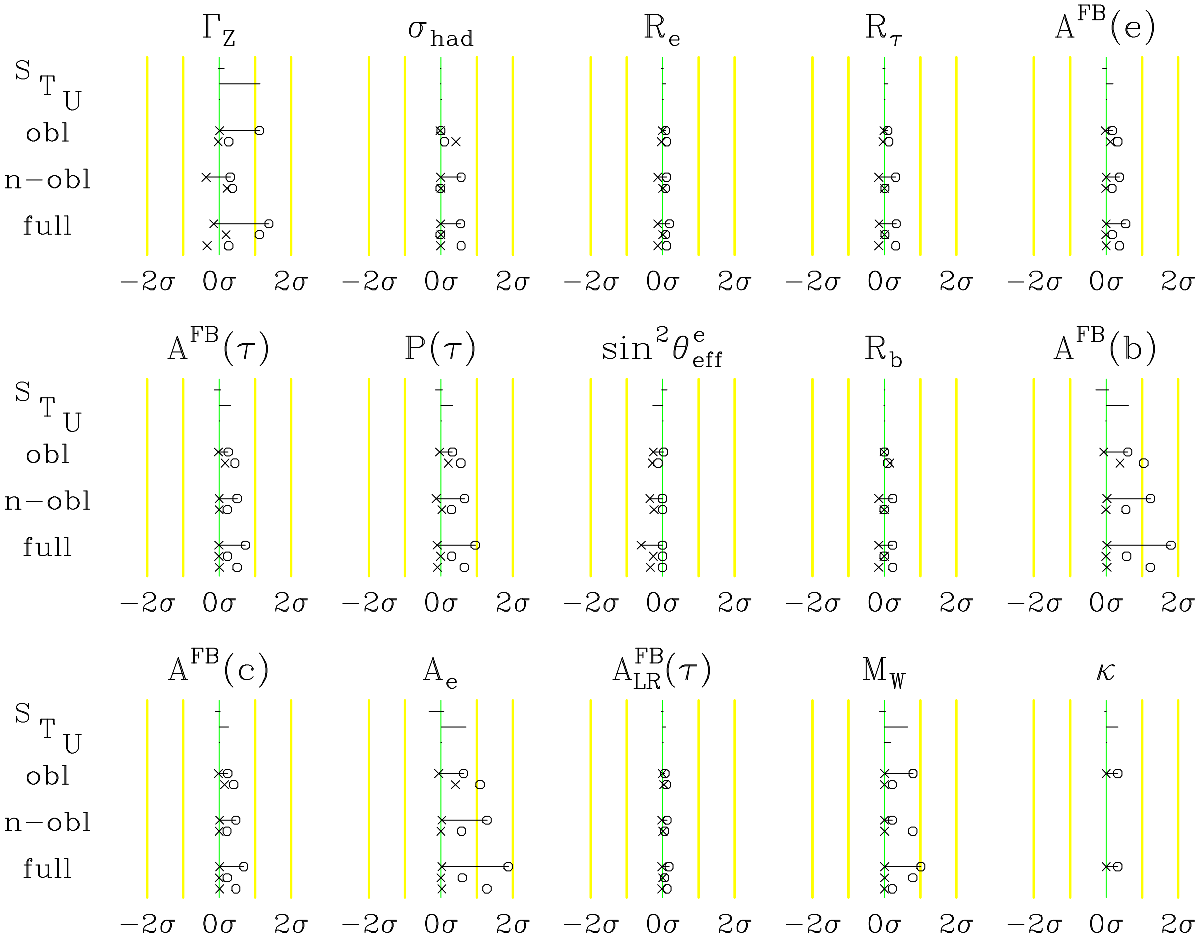

Figure 5: As Fig. 4, for the $\mathbf{5}+\overline{\mathbf{5}}$ gauge-mediated model.

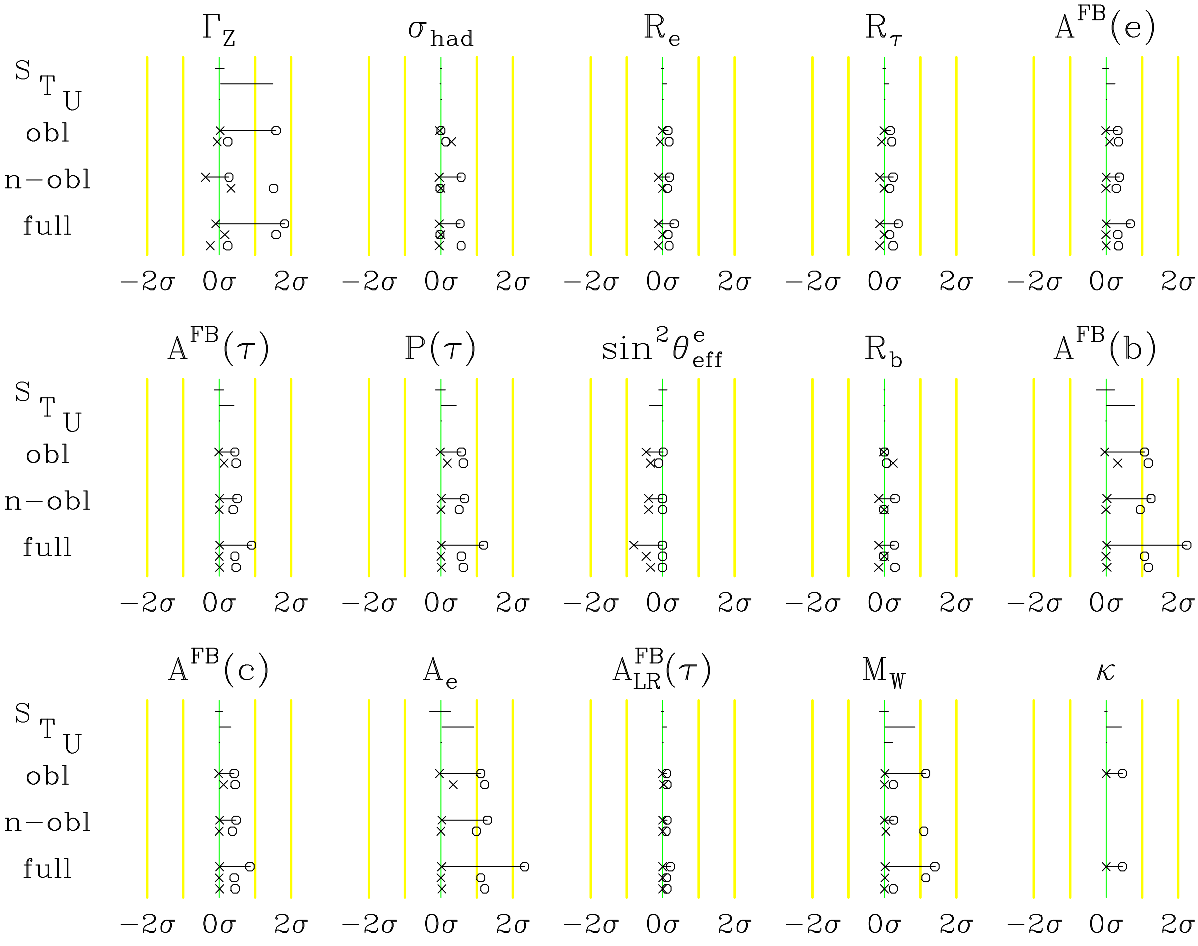

Figure 6: As Fig. 4, for the $\mathbf{10} + \overline{\mathbf{10}}$ gauge-mediated model.

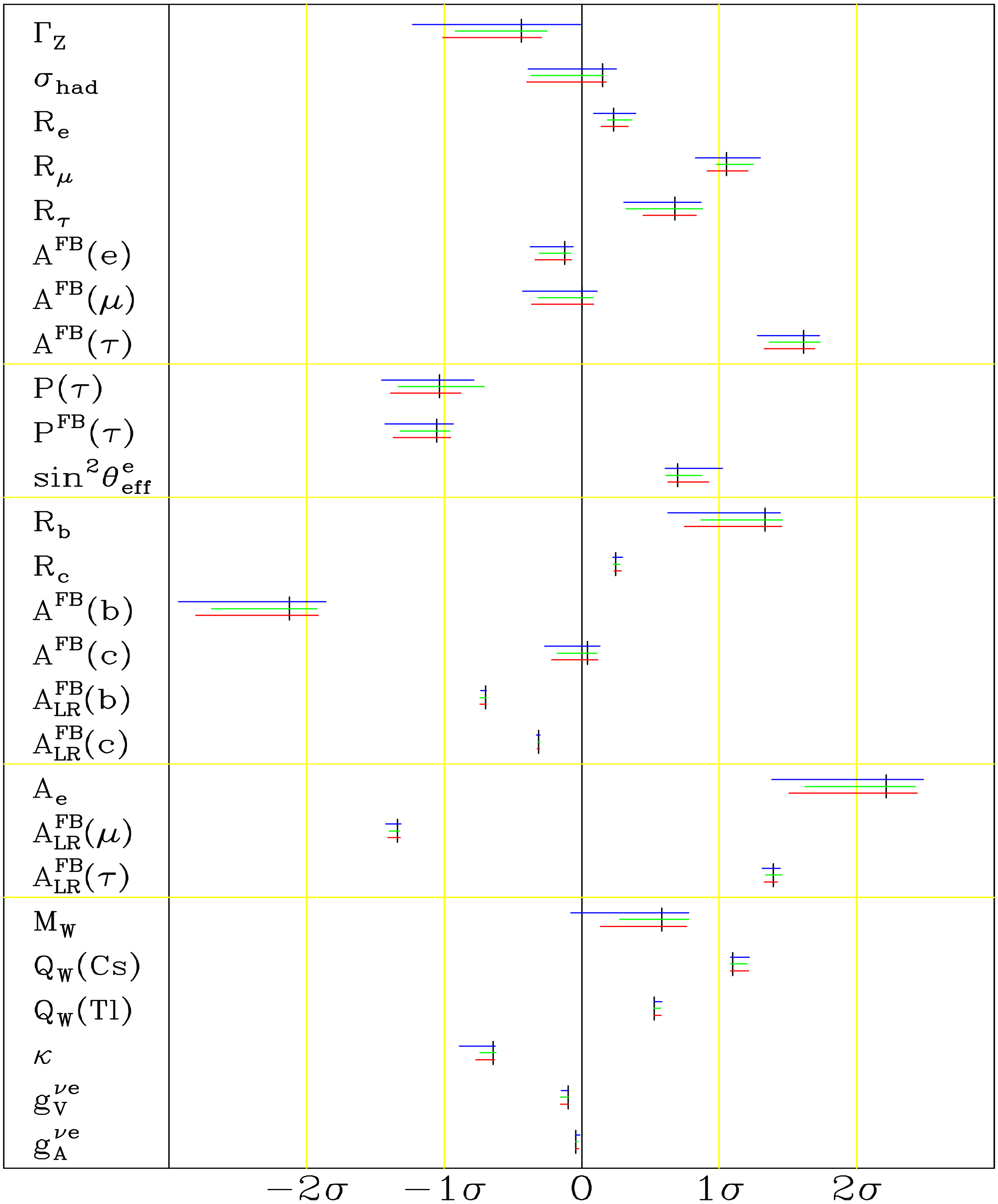

Figure 7: The range of best fit predictions of precision observables in the supergravity model (upper horizontal lines), the $\mathbf{5}+\overline{\mathbf{5}}$ gauge-mediated model (middle lines), the $\mathbf{10}+\overline{\mathbf{10}}$ gauge-mediated model (lower lines), and in the Standard Model at its global best fit value (vertical lines), in units of standard deviation.

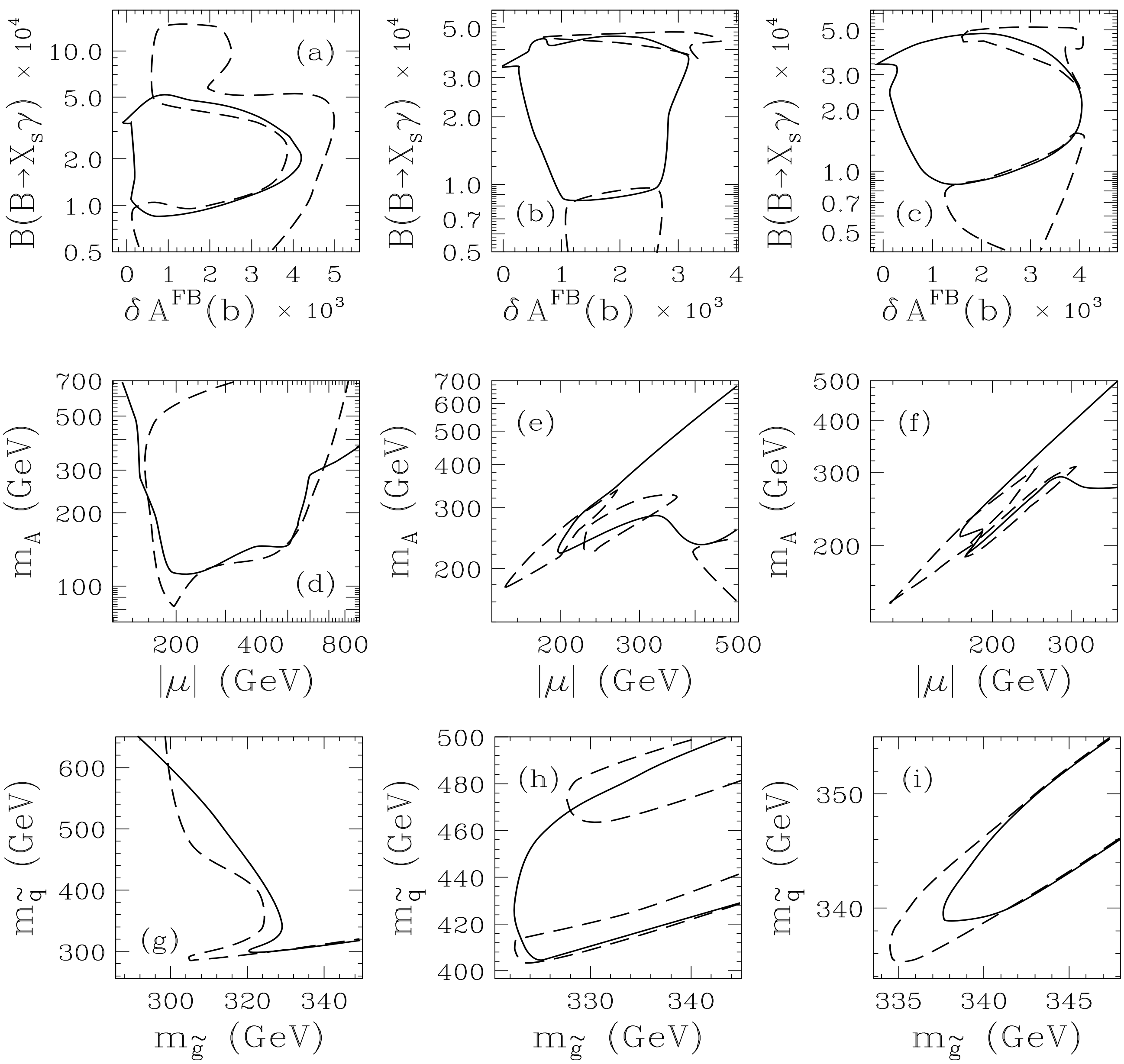

Figure 8: Allowed and excluded regions for various observables and supersymmetry parameters in the minimal supergravity model, and the $\mathbf{5}+\overline{\mathbf{5}}$and $\mathbf{10}+\overline{\mathbf{10}}$ gauge-mediated models (respectively, from left to right), with $\mu < 0$. The regions which contain allowed points lie inside the solid curves, while the regions which contain excluded points are bounded by dashed curves. Therefore, the regions inside dashed curves and outside solid curves are absolutely excluded, independent of the values of other parameters.

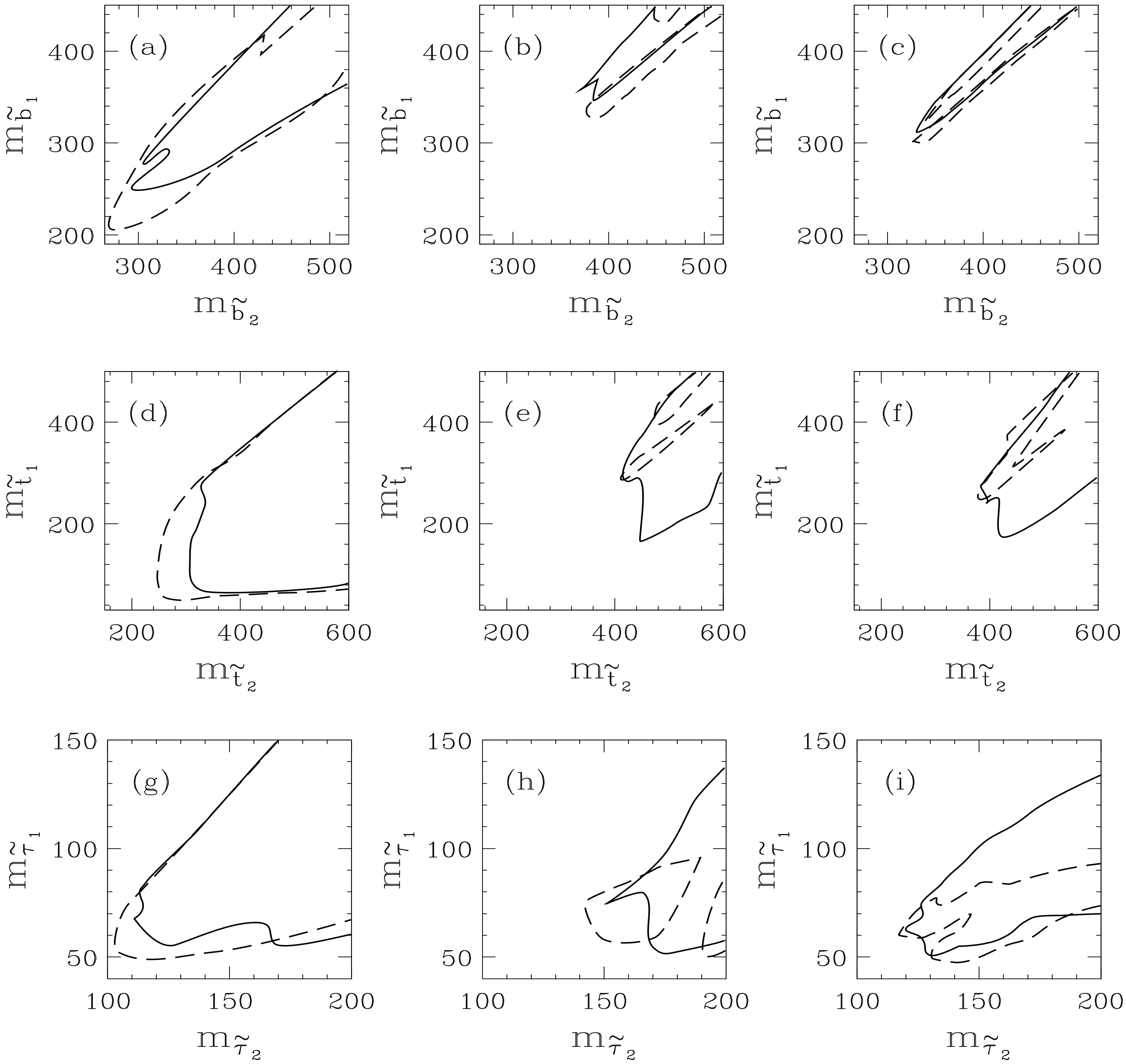

Figure 9: Allowed and excluded $\mu < 0$ regions in third generation squark and slepton mass parameter spaces, as described in Fig. 8. Masses are in GeV.

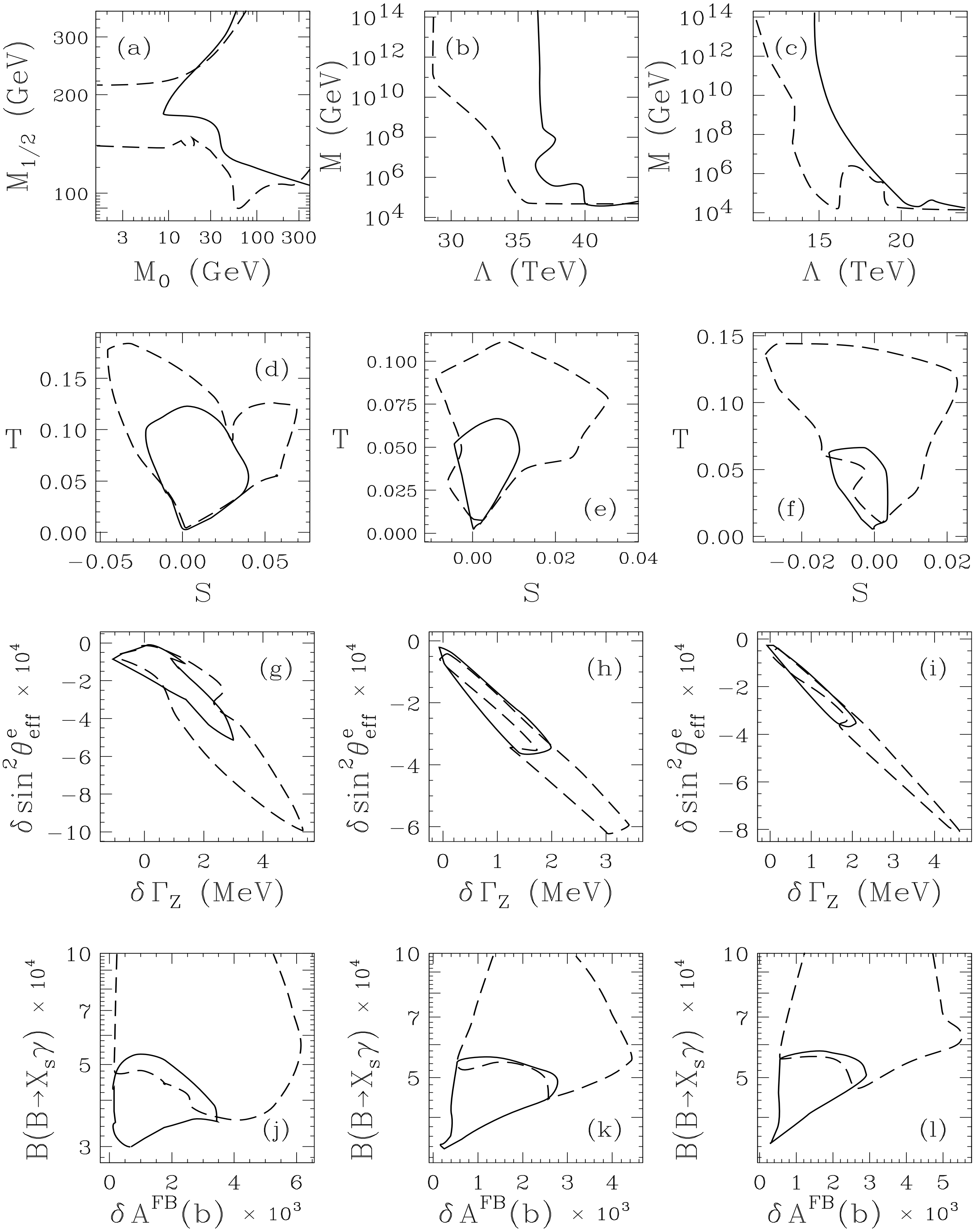

Figure 10: Allowed and excluded regions, as in Fig. 8, with $\mu > 0$.

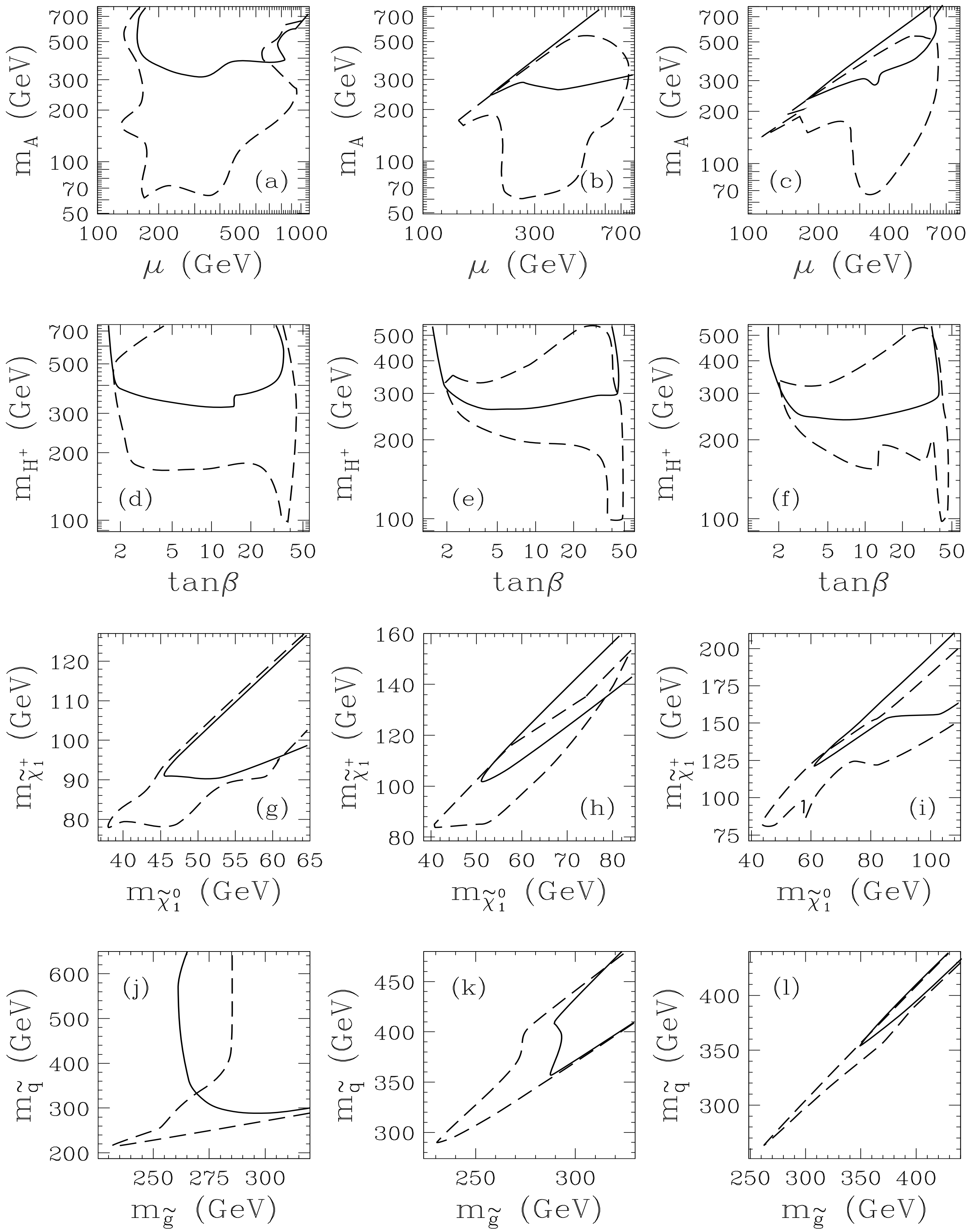

Figure 11: Allowed and excluded regions, as in Fig. 8, with $\mu > 0$.

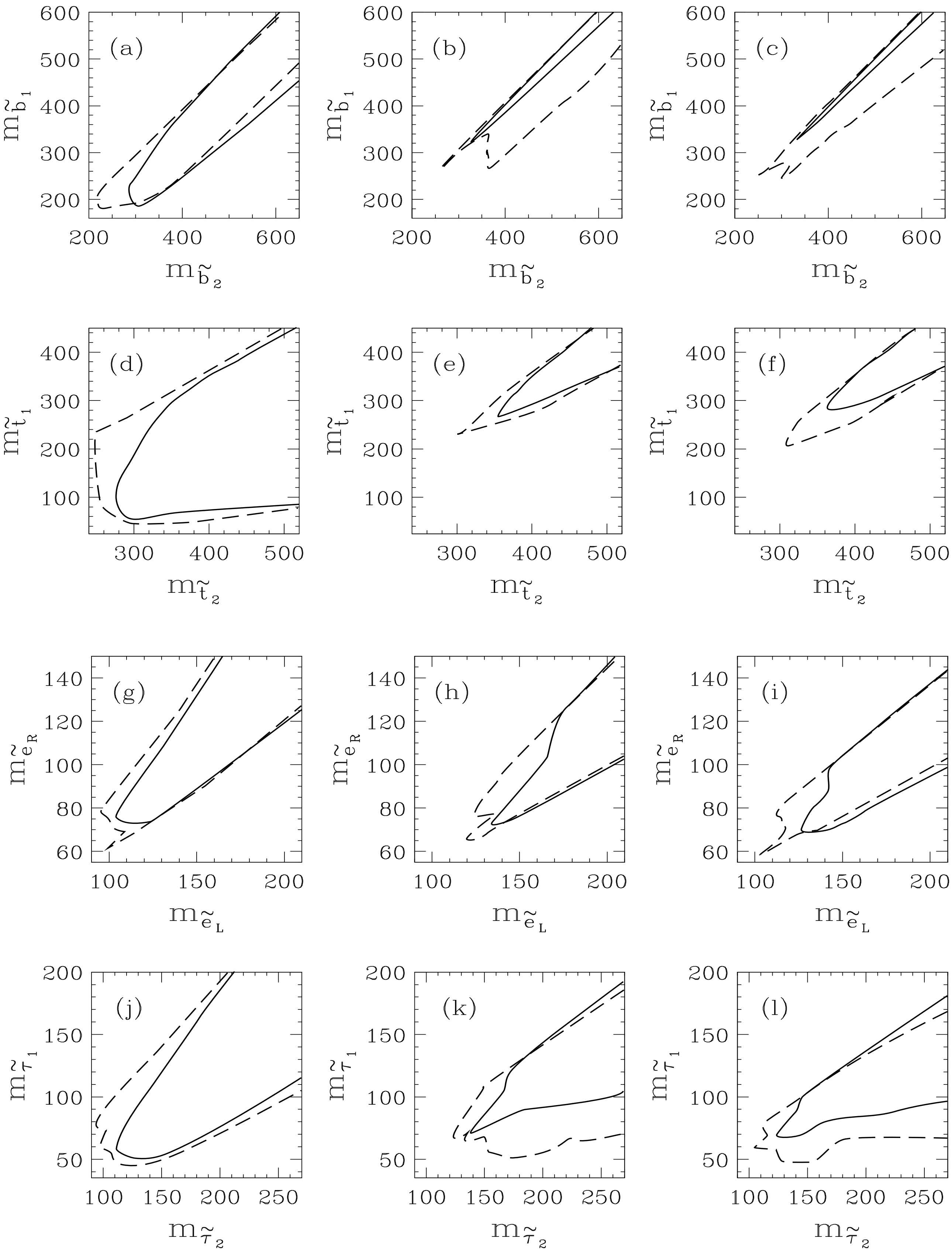

Figure 12: As Fig. 8, in squark and slepton mass parameter spaces, with $\mu > 0$. Masses are in GeV.